

CERN-EP-2023-154
26 July 2023

Modification of charged-particle jets in event-shape engineered Pb–Pb collisions at $\sqrt{s_{\text{NN}}} = 5.02 \text{ TeV}$

ALICE Collaboration*

Abstract

Charged-particle jet yields have been measured in semicentral Pb–Pb collisions at center-of-mass energy per nucleon–nucleon collision $\sqrt{s_{\text{NN}}} = 5.02 \text{ TeV}$ with the ALICE detector at the LHC. These yields are reported as a function of the jet transverse momentum, and further classified by their angle with respect to the event plane and the event shape, characterized by ellipticity, in an effort to study the path-length dependence of jet quenching. Jets were reconstructed at midrapidity from charged-particle tracks using the anti- k_{T} algorithm with resolution parameters $R = 0.2$ and 0.4 , with event-plane angle and event-shape values determined using information from forward scintillating detectors. The results presented in this letter show that, in semicentral Pb–Pb collisions, there is no significant difference between jet yields in predominantly isotropic and elliptical events. However, out-of-plane jets are observed to be more suppressed than in-plane jets. Further, this relative suppression is greater for low transverse momentum ($< 50 \text{ GeV}/c$) $R = 0.2$ jets produced in elliptical events, with out-of-plane to in-plane jet-yield ratios varying up to 5.2σ between different event-shape classes. These results agree with previous studies indicating that jets experience azimuthally anisotropic suppression when traversing the QGP medium, and can provide additional constraints on the path-length dependence of jet energy loss.

*See Appendix A for the list of collaboration members

1 Introduction

At very high energy densities, ordinary hadronic matter undergoes a transition to become a strongly interacting state of deconfined quarks and gluons. This new state of matter is referred to as the quark–gluon plasma (QGP) [1]. Calculations using quantum chromodynamics (QCD) on the lattice predict a crossover transition between these phases at a temperature of about 150 MeV that can be reached in the laboratory via ultrarelativistic collisions of heavy ions [2, 3]. Experimental studies of heavy-ion collisions thus offer a compelling opportunity to explore the properties of the strongly interacting medium, and form the main physics program of the ALICE experiment at the LHC [4].

Jets, sprays of hadrons resulting from high-transverse-momentum (p_T) partons produced in hard-scattering processes, are sensitive to a variety of QGP properties [5–7]. Because jets are produced early in a collision, indeed much earlier than the formation of the QGP at $\tau_{\text{QGP}} \sim 0.5 \text{ fm}/c$, they experience its whole evolution. Jets interact with and are modified by this medium as they traverse it, resulting in a collection of effects known as jet quenching. The observation of jet quenching at both RHIC and LHC energies is therefore considered to be a main signature of QGP formation [8–11], and the microscopic mechanism by which jet quenching occurs has been the subject of significant theoretical and experimental investigation. Models predict that partons can lose energy collisionally and/or radiatively in the weakly-coupled limit, with radiative contributions expected to dominate in the high- p_T regime [12, 13]. Moreover, it is predicted that there is a direct relationship between the path-length dependence of parton energy loss and the relative contributions of the different mechanisms. In a static medium, collisional and radiative energy loss are expected to have a linear and quadratic dependence on the length of plasma traversed, respectively [14, 15]. Measuring this dependence would therefore offer a direct way to probe the underlying mechanisms of jet–medium interactions, but doing so has so far proven to be challenging. Past measurements, e.g. the dijet asymmetry [16–18], are heavily influenced by fluctuations in jet–medium interactions, making it difficult to extract an underlying path-length dependence [19]. Another such measurement, the jet v_2 (the second Fourier coefficient in the azimuthal distribution of jet momenta in the transverse plane), shows a significant azimuthal anisotropy in jet yields in Pb–Pb collisions [20–22]. However, medium fluctuations limit the ability to constrain the underlying physics mechanisms that drive this behavior.

Event-shape engineering (ESE) [23], a technique that classifies events according to their anisotropies using the magnitude of the reduced flow vector, offers a new experimental approach to overcome these difficulties and constrain the path-length dependence of jet energy loss [24]. This approach is advantageous in that it allows for the selection of events for which the thermodynamic properties are similar, but for which the spatial anisotropies vary significantly. This is done by isolating events within a centrality class that have particularly round or elliptical geometries. Previous measurements have shown that the elliptic flow coefficient v_2 of charged particles varies significantly at a fixed collision centrality [25–27]. In addition, the mean p_T of the particle yields is larger for elliptical events than for isotropic events. Results using ESE in the heavy-flavor sector show similar indications [28, 29]. These measurements reveal the sizeable potential that ESE has to connect observables from the soft and hard momentum scales.

Combining the precision afforded by jet measurements with the control that ESE provides to constrain the collision geometry, it is possible to learn about this interplay of physics phenomena from high to low p_T [30]. In the analysis presented in this letter, this interplay is studied by considering an event shape in conjunction with the jet angle with respect to the event-plane Ψ_2 , which is defined by the beam axis and the vector of the collision impact parameter. The distance the jet traverses through the medium when traveling parallel to the event plane (in-plane) is, on average, shorter than when it travels perpendicular to the event plane (out-of-plane). As such, the azimuthal anisotropy of the jet spectra provides initial information about the path-length dependence of parton energy loss. By then applying ESE, the relative difference between in- and out-of-plane jet path-lengths can be increased or decreased. This is especially true in the case of semicentral collisions, where the system is usually (but not necessarily) elliptical. In

semicentral Pb–Pb collisions at $\sqrt{s_{\text{NN}}} = 2.76$ TeV, the charged-particle v_2 ratio for the 30% most elliptical events compared to the 30% most isotropic events is ~ 1.3 [26]. This ratio was approximated by considering the average of the charged-particle v_2 values reported in differentiated centrality and ellipticity windows. With this in consideration, comparing in- and out-of-plane jet spectra for events with different ellipticities can reduce the contribution of medium shape fluctuations and increase understanding of the path-length dependence of jet energy loss.

In this letter, results of event-shape engineered jet yields in 30–50% Pb–Pb collisions at $\sqrt{s_{\text{NN}}} = 5.02$ TeV are presented. Jets were reconstructed from charged-particle tracks for resolution parameters $R = 0.2$ and $R = 0.4$, within a jet transverse-momentum range of $35 < p_{\text{T},\text{ch jet}} < 120$ GeV/ c and $40 < p_{\text{T},\text{ch jet}} < 120$ GeV/ c , respectively. The in-plane and out-of-plane jet yields are presented according to the ellipticity of the collision system quantified event-by-event, which allows for the exploitation of average differences in jet path length.

2 Experimental Setup

The ALICE experiment is a general-purpose detector located at the LHC. It is optimized to provide high momentum resolution and excellent particle identification over a broad momentum range, up to the highest multiplicities [31]. The primary ALICE sub-detectors used in this analysis are the Inner Tracking System (ITS), Time Projection Chamber (TPC), and V0 detectors. For more information on the ALICE apparatus and its performance, see Refs. [32, 33].

The ITS is a silicon-based tracking detector used for reconstruction of charged tracks and primary vertex identification [34]. It consists of six layers having increasing radii around the nominal collision point. The first two layers are Silicon Pixel Detectors (SPD), followed by two layers of Silicon Drift Detectors (SDD), and two layers of Silicon Strip Detectors (SSD). The TPC is a large cylindrical gaseous detector, covering a pseudorapidity range of $|\eta| < 0.9$ over the full azimuthal angle [35] and providing excellent tracking performance up to high particle multiplicities and momenta. The tracks used for jet reconstruction in this analysis were measured by both the ITS and the TPC, and were accepted for $p_{\text{T}} > 0.15$ GeV/ c and pseudorapidities of $|\eta| < 0.9$. The tracks have a momentum resolution of $\sigma_{p_{\text{T}}}/p_{\text{T}} \sim 0.8\%$ at $p_{\text{T}} = 1$ GeV/ c , which increases to $\sigma_{p_{\text{T}}}/p_{\text{T}} \sim 2\%$ at $p_{\text{T}} = 10$ GeV/ c [33]. In central Pb–Pb collisions, the tracking efficiency ranges from approximately 65% to 82% for increasing p_{T} [8].

The V0A and V0C, scintillation detectors located at pseudorapidities $2.8 < \eta < 5.1$ and $-3.7 < \eta < -1.7$, respectively, were used to select the Pb–Pb minimum-bias and semicentral events according to their summed amplitudes [36, 37]. In this analysis, the V0C was used for calculating the reduced flow vector q_2 , defined in Eq. 1, as it is closer to midrapidity than the V0A. It can therefore produce a wider q_2 distribution, thus accessing the best separation between different event shapes. The V0A was used for calculating event-plane angles to minimize autocorrelations between charged-particle jets at midrapidity and the event-shape determination at more forward rapidity. Details of the q_2 and event-plane angle measurements are given in the next section.

3 Data Analysis

The results presented in this letter are derived from a sample of Pb–Pb collisions collected by the ALICE experiment during the 2018 LHC heavy-ion run. The data sample considered in this work was recorded with a semicentral trigger based on the V0 signal amplitude, which allowed for the collection of a large sample of Pb–Pb collisions in the 30–50% centrality class [31]. Only events having a primary vertex within ± 10 cm of the nominal interaction point along the beam line (z direction) were accepted. An additional selection criterion was applied to remove pile-up, utilizing the correlation between the number of hits in the ITS and TPC detectors. After applying these criteria, a total of approximately 54 million

events were selected for this study.

Jets were reconstructed from charged-particle tracks [38] with the FastJet anti- k_T algorithm [39, 40]. The p_T -scheme recombination strategy was chosen to combine tracks using their transverse momenta [39, 41]. The resolution parameters $R = 0.2$ and $R = 0.4$ were studied, where each jet was required to contain a leading track with $5 < p_T < 100$ GeV/c. The leading track requirement was chosen to reduce contamination from combinatorial jets. The jet axis was required to be within $|\eta_{\text{jet}}| < 0.9 - R$, where η_{jet} is the pseudorapidity of the jet axis. Furthermore, for each jet the quantity $\Delta\varphi = \varphi_{\text{jet}} - \Psi_2$ was calculated. This is the difference in azimuthal angle between the jet axis and the event-plane angle Ψ_2 , where Ψ_2 is determined from the V0A signals. The average combinatorial background was subtracted using an area-based technique [38, 42, 43]. With this method, the background transverse-momentum density per unit area, ρ , was determined event-by-event after removing the two leading k_T jets [44]. The jet energies were corrected for the underlying-event contribution by subtracting the event-averaged density multiplied by the jet area. The residual background fluctuations, together with detector effects, were then corrected on a statistical basis using a 2D Bayesian unfolding procedure [45, 46]. The choice to use a 2D procedure was made so as to correct for the differences in background arising from the jet angle with respect to Ψ_2 , as well as to account for any correlated bin migration in $\Delta\varphi$ and $p_{T,\text{chjet}}$. This was done using a 4D response matrix constructed from PYTHIA 8 (Monash tune) [47, 48] jets transported through the ALICE detector by a GEANT3-based simulation [49] and embedded into real Pb–Pb events. The data was binned in $p_{T,\text{chjet}}$ and $|\cos(\Delta\varphi)|$ for both truth- and reconstructed-level jets. Before filling the response matrix, 2% of simulated tracks were randomly rejected before jet-finding to account for the worsened tracking efficiency in the high track-density environment of Pb–Pb collisions. This level of degradation was estimated using HIJING simulations of 0–10% central Pb–Pb collisions [50]. The 2D jet distribution was then unfolded using six iterations of the Bayesian procedure, with the PYTHIA 8 distribution used as the prior.

After unfolding, corrections were applied to the jet yields for the kinematic and reconstruction efficiencies. Here, the kinematic efficiency refers to the inefficiency introduced by truth-level jets that were reconstructed outside of the measured $p_{T,\text{chjet}}$ range, thus not entering the unfolding procedure. This was computed for each bin by taking the ratio of the truth-level spectrum reconstructed in the measured range to the truth level-spectrum reconstructed within $10 < p_{T,\text{chjet}} < 200$ GeV/c. The reconstruction efficiency accounts for truth-level jets that were not found at detector-level. Corrections were also applied to account for the event-plane resolution when the event-plane angle was considered. The reported $p_{T,\text{chjet}}$ ranges are 35–120 GeV/c and 40–120 GeV/c for $R = 0.2$ and $R = 0.4$ jets, respectively. These ranges were chosen to satisfy the requirement of having a kinematic efficiency above 75% for each generator-level $p_{T,\text{chjet}}$ bin, as well as to ensure stability when varying the lower limit of the $p_{T,\text{chjet}}$ range considered in the unfolding procedure.

To study the event-shape dependence, events were classified according to the magnitude of the reduced flow vector q_2 [51] as measured with the V0C, defined as

$$q_2 = |\mathbf{Q}_2|/\sqrt{M}, \quad (1)$$

where M represents the charged-particle multiplicity and \mathbf{Q}_2 represents the second harmonic flow vector, defined as

$$\mathbf{Q}_2 = \left(\sum_i w_i \cos(2\varphi_i), \sum_i w_i \sin(2\varphi_i) \right). \quad (2)$$

Here, φ_i and w_i are the azimuthal angle and signal weight, respectively, of the i -th segment of the V0C detector [33, 52]. Samples of events with the 30% smallest and largest q_2 were selected for this study and will be henceforth referred to as q_2 -small and q_2 -large. These designations represent isotropic and elliptical event topologies, respectively. Figure 1 shows the distribution of q_2 values as a function of collision centrality in Pb–Pb collisions at $\sqrt{s_{\text{NN}}} = 5.02$ TeV. The pink lines demarcate the 30th and 70th

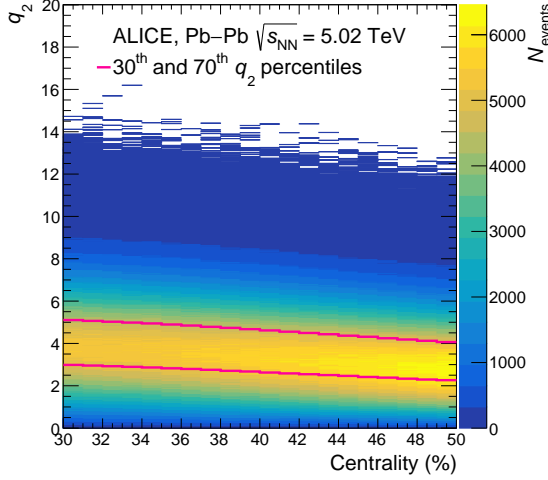


Figure 1: Distribution of q_2 values as a function of centrality in Pb–Pb collisions at $\sqrt{s_{\text{NN}}} = 5.02 \text{ TeV}$. Pink lines demarcate the 30th and 70th q_2 percentiles, as calculated within 1%-wide centrality intervals.

percentiles in q_2 . Note that the q_2 -small sample contains a significant fraction of events with non-zero v_2 , so, while this sample is characterized as comparatively isotropic, there still exists some significant anisotropy within the sample. The slope of the distribution indicates that the average values of q_2 are slightly larger for more central collisions, which can introduce a centrality bias in the event class selection. To avoid this correlation bias, the q_2 classification was done within 1%-wide centrality intervals.

The event-plane angle Ψ_2 , given by the direction of \mathbf{Q}_2 , was measured with the V0A detector. The in- and out-of-plane axes were defined as parallel and perpendicular to Ψ_2 , respectively. Jets were considered in- and out-of-plane when they were reconstructed within 30° in azimuth of these axes. This restriction from the traditional $\pm 45^\circ$ definition was made to enforce larger differences between in- and out-of-plane path lengths and to increase the potential differences in jet yields [30]. The use of opposed detectors for q_2 and Ψ_2 is advantageous for avoiding autocorrelations between these observables and for reducing detector-resolution corrections.

To account for the smearing of the reaction-plane angle due to the event-plane resolution, the ratios of in- and out-of-plane jet yields were corrected using a procedure analogous to that used for v_2 measurements [53]. First, the v_2 was calculated using

$$v_2 = \frac{\pi}{3\sqrt{3}} R_2 \frac{N_{\text{in}} - N_{\text{out}}}{N_{\text{in}} + N_{\text{out}}}, \quad (3)$$

where R_2 is the second harmonic event-plane resolution, and N_{in} and N_{out} are the in- and out-of-plane jet yields, respectively. Note that the coefficient $\pi/(3\sqrt{3})$ in this formula is specific to this analysis, in which the in- and out-of-plane definitions are at $\pm 30^\circ$ around Ψ_2 and the vector perpendicular to it, as described above. The event-plane resolution R_2 was calculated using the three-sub-event method [53], where the particles measured by the V0A, V0C, and TPC detectors were used to construct the three separate sub-events. For q_2 -small samples, R_2 is 0.55, whereas for q_2 -large samples it is 0.68. After calculating the corrected v_2 , the corrected ratio $\mathcal{R} = N_{\text{out}}/N_{\text{in}}$ was obtained by inverting Eq. 3 and assuming a perfect resolution $R_2 = 1$. To correct the individual spectra for the event-plane resolution, conservation of jet yields within the fiducial volume ($N_{\text{in}}^{\text{measured}} + N_{\text{out}}^{\text{measured}} = N_{\text{in}}^{\text{corrected}} + N_{\text{out}}^{\text{corrected}}$) was additionally considered, such that

Table 1: Relative systematic uncertainties for the charged-particle jet yields as measured in 30–50% Pb–Pb collisions at $\sqrt{s_{\text{NN}}} = 5.02$ TeV. Values are reported as percentages. Reported ranges reflect the minimum and maximum values of the uncertainties over the measured $p_{\text{T},\text{chjet}}$ range. Here, < 1 indicates an uncertainty with a decimal value greater than zero but less than one.

	$R = 0.2$				$R = 0.4$			
	q_2 -small		q_2 -large		q_2 -small		q_2 -large	
	in-plane	out-of-plane	in-plane	out-of-plane	in-plane	out-of-plane	in-plane	out-of-plane
Tracking efficiency	6–15	6–12	8–10	6–16	4–15	6–15	6–20	<1–17
Unfolding iterations	<1	<1	<1	<1	<1–2	<1–4	1–3	<1–3
Unfolding prior	<1–3	<1–2	<1–2	<1–2	2–6	<1–5	<1–8	2–5
Unfolding truncation	<1	<1	<1	<1	<1–10	<1–7	1–13	<1–9
Event-plane determination	<1	<1	<1	<1	<1	<1	<1	<1
Total	6–15	6–12	8–10	6–16	8–16	6–16	12–21	9–17

$$N_{\text{in}}^{\text{corrected}} = \frac{N_{\text{in}}^{\text{measured}} + N_{\text{out}}^{\text{measured}}}{1 + \mathcal{R}}, \quad N_{\text{out}}^{\text{corrected}} = \frac{N_{\text{in}}^{\text{measured}} + N_{\text{out}}^{\text{measured}}}{1 + 1/\mathcal{R}}. \quad (4)$$

For the ratio of out-of-plane to in-plane jet yields, the magnitude of this correction varies from 5 to 25%. Note that N_{mid} remains unmodified, where N_{mid} is the jet yield reconstructed between $\pm 30^\circ - 60^\circ$ of the event plane. This correction procedure is exact when assuming a negligible contribution from higher order harmonics. Additionally, the contribution of non-flow to the measured yield ratios was estimated using PYTHIA 8. Here, non-flow refers to the v_2 contribution from forward multi-jets that result in a biased determination of Ψ_2 . It was found that, for cases where an intermediate $p_{\text{T},\text{chjet}}$ jet is produced at midrapidity, a recoiling jet strikes the VOA in < 4% of instances. The relative contribution from these events to the jet v_2 is estimated to be less than 20%. The presented results are not corrected for this possible effect.

The systematic uncertainties of the charged-particle jet yields and their ratios are summarized in Tables 1 and 2, respectively. The ranges of systematic uncertainties are listed for the measured $p_{\text{T},\text{chjet}}$ range. The systematic uncertainty on the tracking efficiency was calculated by randomly rejecting an additional 4% of PYTHIA 8 tracks used in the embedding procedure, representing the uncertainty in the single-track efficiency in the Pb–Pb environment. The jet finding was then repeated and the response matrix recalculated, resulting in the largest source of uncertainty for the measured spectra. The uncertainty in the unfolding procedure was quantified by varying the number of iterations of unfolding, the shape of the prior $p_{\text{T},\text{chjet}}$ and $\Delta\phi$ spectra, and the lower limit of the measured range (referred to as the truncation). The shape variation was done by reweighting the unfolding prior according to the ratio between the PYTHIA 8 and data spectra in both $p_{\text{T},\text{chjet}}$ and event-plane angle. The number of unfolding iterations was varied by ± 1 . The lower $p_{\text{T},\text{chjet}}$ limit for the jets that entered into the unfolding procedure was varied by ± 5 GeV/c. Finally, the systematic uncertainty of the event-plane resolution was obtained by varying R_2 by 2%. This 2% variation accounts for the difference in event-plane resolution observed when it is calculated using the χ -ratio method as opposed to the three-sub-event method [26, 53]. Note that this uncertainty is only considered for the measurements that are differentiated in $\Delta\phi$. For the ratios of the spectra, the systematic uncertainties in the numerator and denominator were treated as correlated, and the resulting systematic uncertainty was obtained by making the above-described variations and calculating the deviations on the ratio itself. The total systematic uncertainties were calculated as quadratic sums of the different sources by assuming the independence of all contributions.

Table 2: Relative systematic uncertainties for the ratios of charged-particle jet yields as measured in 30–50% Pb–Pb collisions at $\sqrt{s_{\text{NN}}} = 5.02$ TeV. Values are reported as percentages. Reported ranges reflect the minimum and maximum values of the uncertainties over the measured $p_{T,\text{ch jet}}$ range. Here, < 1 indicates an uncertainty with a decimal value greater than zero but less than one.

	$R = 0.2$			$R = 0.4$		
	$q_2\text{-large}/q_2\text{-small}$	$q_2\text{-small}$ out-/in-plane	$q_2\text{-large}$ out-/in-plane	$q_2\text{-large}/q_2\text{-small}$	$q_2\text{-small}$ out-/in-plane	$q_2\text{-large}$ out-/in-plane
Tracking efficiency	1–3	<1–2	<1–5	1–3	4–9	1–9
Unfolding iterations	<1	<1	<1	<1	<1–6	2–6
Unfolding prior	<1–3	<1–2	<1–3	<1–3	1–5	<1–12
Unfolding truncation	<1	<1	<1	<1–3	1–18	1–21
Event-plane determination	N/A	<1	<1	N/A	<1	<1
Total	1–4	2–3	1–5	1–5	5–21	4–25

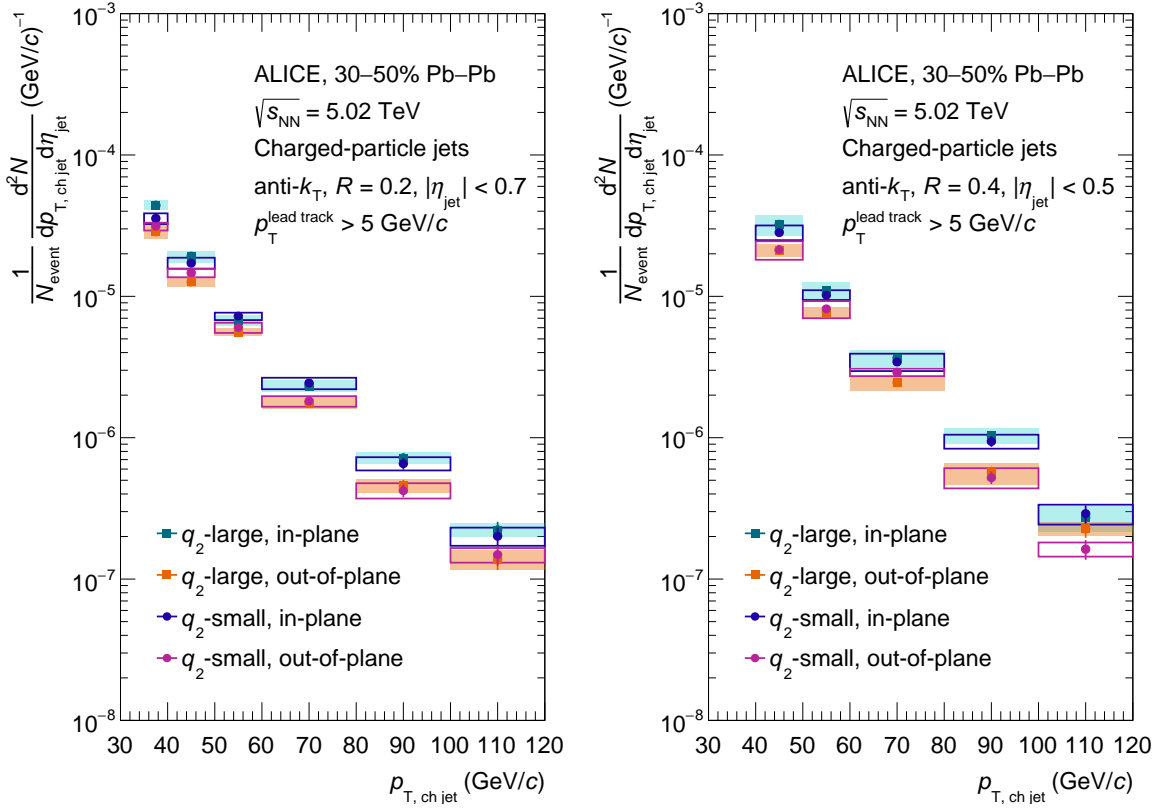


Figure 2: Charged-particle jet yields for $R = 0.2$ (left) and $R = 0.4$ (right) jets in Pb–Pb collisions at $\sqrt{s_{\text{NN}}} = 5.02$ TeV. Results are shown for the $q_2\text{-small}$ and $q_2\text{-large}$ event classes, for in- and out-of-plane jets. The bars (boxes) represent statistical (systematic) point-by-point uncertainties.

4 Results

The $p_{T,\text{ch jet}}$ -differential charged-particle jet yields for resolution parameters $R = 0.2$ and $R = 0.4$ are shown in Fig. 2. Included are the results for the event classes $q_2\text{-small}$ and $q_2\text{-large}$, differentiated for in-plane and out-of-plane jets. The systematic uncertainties are indicated by the boxes and are highly correlated among the different measurements.

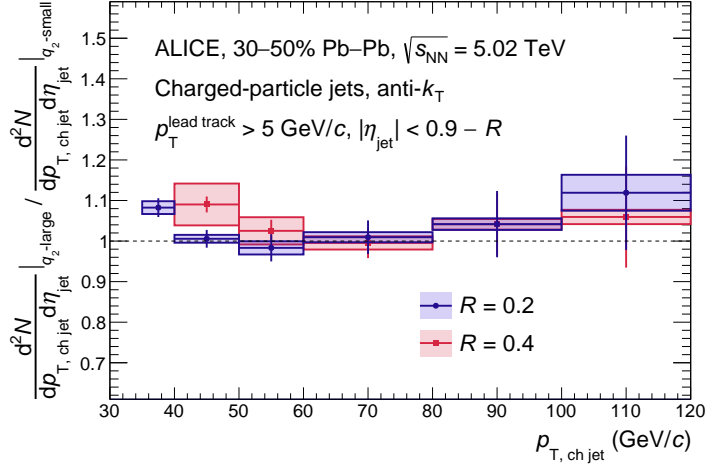


Figure 3: Ratio of the charged-particle jet yields of the q_2 -large to the q_2 -small event classes, in Pb–Pb collisions at $\sqrt{s_{\text{NN}}} = 5.02 \text{ TeV}$. The results are reported for $R = 0.2$ and $R = 0.4$ jets.

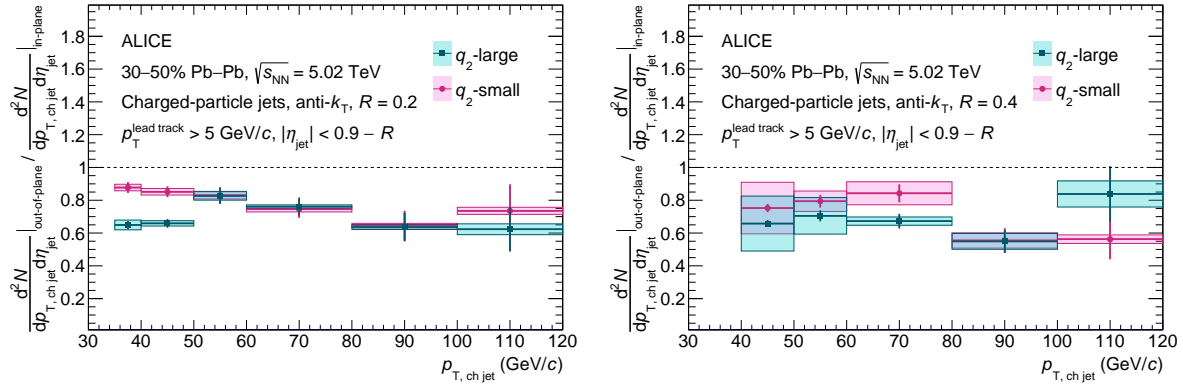


Figure 4: Ratios of out-of-plane to in-plane charged-particle jet yields for the q_2 -large and q_2 -small event classes in Pb–Pb collisions at $\sqrt{s_{\text{NN}}} = 5.02 \text{ TeV}$. The results are reported for $R = 0.2$ (left) and $R = 0.4$ (right) jets, and are corrected for the event-plane resolution.

The ratios of charged-particle jet yields for the q_2 -large to q_2 -small event classes are shown in Fig. 3, for both $R = 0.2$ and $R = 0.4$. Considering these results as ratios allowed for a reduction in the systematic uncertainties due to correlations of the uncertainties between the spectra, thus improving the sensitivity of this measurement. The results are consistent with unity, indicating that azimuthally-integrated jet yields are not sensitive to collision ellipticity. This stands in contrast to the yield enhancement seen in elliptical collisions at low p_T [25], where particle spectra are not governed by quenching, but rather by the hydrodynamic expansion of the medium.

Figure 4 shows the ratio of out-of-plane to in-plane jet yields for the q_2 -small and q_2 -large event classes, for jets with $R = 0.2$ (left) and $R = 0.4$ (right). These results were corrected for the event-plane resolution, as described in the previous section. The measured ratios are significantly below unity, indicating that jets lose more energy on average when traveling out-of-plane than when traveling in-plane. This is consistent with the idea that the magnitude of jet energy loss is driven, at least in part, by the path length traversed in the medium. For $R = 0.4$ jets, further conclusions regarding event-shape dependent azimuthal anisotropy

are limited by the large experimental uncertainties. For $R = 0.2$ jets, the ratios for q_2 -small and q_2 -large are similar at high $p_{T,\text{chjet}}$. For $p_{T,\text{chjet}} < 50 \text{ GeV}/c$, however, there is an indication that out-of-plane jets in the q_2 -large class are more suppressed relative to in-plane jets than those in the q_2 -small class. The significance of this separation from $35 < p_{T,\text{chjet}} < 50 \text{ GeV}/c$ is 5.2σ . This result is qualitatively in agreement with observations of D mesons [29].

This effect is expected due to the increased path-length differences between in- and out-of-plane directions for highly elliptical collision geometries, which is supported by Trajectum calculations [30, 54]. In these calculations, probes were generated in the initial state at the location of nucleon–nucleon collisions, and propagated through the hydrodynamically evolving medium while remaining unmodified. The average path lengths of these probes were calculated for events with varying q_2 , and differentially for in- and out-of-plane emission angles. While the results of this study show that the average traversed path length of the probes does not vary significantly with event q_2 , it does change as a function of the probe angle with respect to Ψ_2 . This variation with Ψ_2 can be further augmented when considering q_2 -large events, and suppressed when considering q_2 -small events. The outcome of these Trajectum calculations shows that by using ESE, the ratio of out-of-plane to in-plane path lengths can be increased in semicentral collisions by $\sim 10\%$ with respect to the inclusive case. The results presented in this letter are consistent with these calculations, assuming that the traversed path length of jets is an important factor for determining their energy loss. These Trajectum studies do not, however, allow one to conclude anything about the $p_{T,\text{chjet}}$ -dependence of this energy loss or explain the apparent convergence of ratios at high $p_{T,\text{chjet}}$. Despite the absence of phenomenological descriptions, a possible understanding of the experimental results at high $p_{T,\text{chjet}}$ can be obtained by considering that the charged-particle jet R_{AA} increases and the charged-particle jet v_2 decreases with increasing $p_{T,\text{chjet}}$ [20, 55]. It is therefore expected that any path-length-dependent signal accessible to ESE measurements would decrease at high $p_{T,\text{chjet}}$. Moreover, the precision of the measurement presented here is statistically limited at high $p_{T,\text{chjet}}$. It is therefore difficult to establish if the convergence of out-of-plane to in-plane ratios for elliptical and isotropic events is a true physics phenomenon, or is rather a consequence of the limited experimental precision accessible at high $p_{T,\text{chjet}}$.

This measurement demonstrates the potential of the ESE technique and paves the way for future studies with larger data samples. However, a full interpretation of these results requires detailed comparisons to model calculations, which will allow for more quantitative conclusions on the path-length dependence of energy loss.

5 Conclusions

In this letter, the measured event-shape engineered jet yields are reported for resolution parameters $R = 0.2$ and $R = 0.4$ in semicentral Pb–Pb collisions at $\sqrt{s_{\text{NN}}} = 5.02 \text{ TeV}$. The magnitude of the reduced second harmonic flow vector q_2 was used to select event classes that are particularly isotropic (q_2 -small) and elliptical (q_2 -large). The jet spectra from these two event classes are consistent within their uncertainties. However, a significant deviation between jet spectra is observed when these jets are classified according to their azimuthal angle with respect to the event plane. It is indicated that jets lose more energy out-of-plane compared to in-plane, consistent with the measurement of a non-zero v_2 of jets at the LHC. Furthermore, for $R = 0.2$ jets in highly elliptical events, the differences between the modification of out-of-plane and in-plane jets at low $p_{T,\text{chjet}}$ are found to be more significant than in more isotropic events. Model calculations employing a realistic parton shower in event-by-event hydrodynamical simulations, such as LBT [56, 57], JETSCAPE [58], or JEWEL on a (2+1)D background [59, 60], are needed to further interpret these results and gain insight into the path-length dependence of jet quenching.

Acknowledgements

The ALICE Collaboration would like to thank all its engineers and technicians for their invaluable contributions to the construction of the experiment and the CERN accelerator teams for the outstanding performance of the LHC complex. The ALICE Collaboration gratefully acknowledges the resources and support provided by all Grid centres and the Worldwide LHC Computing Grid (WLCG) collaboration. The ALICE Collaboration acknowledges the following funding agencies for their support in building and running the ALICE detector: A. I. Alikhanyan National Science Laboratory (Yerevan Physics Institute) Foundation (ANSL), State Committee of Science and World Federation of Scientists (WFS), Armenia; Austrian Academy of Sciences, Austrian Science Fund (FWF): [M 2467-N36] and Nationalstiftung für Forschung, Technologie und Entwicklung, Austria; Ministry of Communications and High Technologies, National Nuclear Research Center, Azerbaijan; Conselho Nacional de Desenvolvimento Científico e Tecnológico (CNPq), Financiadora de Estudos e Projetos (Finep), Fundação de Amparo à Pesquisa do Estado de São Paulo (FAPESP) and Universidade Federal do Rio Grande do Sul (UFRGS), Brazil; Bulgarian Ministry of Education and Science, within the National Roadmap for Research Infrastructures 2020-2027 (object CERN), Bulgaria; Ministry of Education of China (MOEC), Ministry of Science & Technology of China (MSTC) and National Natural Science Foundation of China (NSFC), China; Ministry of Science and Education and Croatian Science Foundation, Croatia; Centro de Aplicaciones Tecnológicas y Desarrollo Nuclear (CEADEN), Cubaenergía, Cuba; Ministry of Education, Youth and Sports of the Czech Republic, Czech Republic; The Danish Council for Independent Research — Natural Sciences, the VILLUM FONDEN and Danish National Research Foundation (DNRF), Denmark; Helsinki Institute of Physics (HIP), Finland; Commissariat à l’Energie Atomique (CEA) and Institut National de Physique Nucléaire et de Physique des Particules (IN2P3) and Centre National de la Recherche Scientifique (CNRS), France; Bundesministerium für Bildung und Forschung (BMBF) and GSI Helmholtzzentrum für Schwerionenforschung GmbH, Germany; General Secretariat for Research and Technology, Ministry of Education, Research and Religions, Greece; National Research, Development and Innovation Office, Hungary; Department of Atomic Energy Government of India (DAE), Department of Science and Technology, Government of India (DST), University Grants Commission, Government of India (UGC) and Council of Scientific and Industrial Research (CSIR), India; National Research and Innovation Agency - BRIN, Indonesia; Istituto Nazionale di Fisica Nucleare (INFN), Italy; Japanese Ministry of Education, Culture, Sports, Science and Technology (MEXT) and Japan Society for the Promotion of Science (JSPS) KAKENHI, Japan; Consejo Nacional de Ciencia (CONACYT) y Tecnología, through Fondo de Cooperación Internacional en Ciencia y Tecnología (FONCICYT) and Dirección General de Asuntos del Personal Académico (DGAPA), Mexico; Nederlandse Organisatie voor Wetenschappelijk Onderzoek (NWO), Netherlands; The Research Council of Norway, Norway; Commission on Science and Technology for Sustainable Development in the South (COMSATS), Pakistan; Pontificia Universidad Católica del Perú, Peru; Ministry of Education and Science, National Science Centre and WUT ID-UB, Poland; Korea Institute of Science and Technology Information and National Research Foundation of Korea (NRF), Republic of Korea; Ministry of Education and Scientific Research, Institute of Atomic Physics, Ministry of Research and Innovation and Institute of Atomic Physics and University Politehnica of Bucharest, Romania; Ministry of Education, Science, Research and Sport of the Slovak Republic, Slovakia; National Research Foundation of South Africa, South Africa; Swedish Research Council (VR) and Knut & Alice Wallenberg Foundation (KAW), Sweden; European Organization for Nuclear Research, Switzerland; Suranaree University of Technology (SUT), National Science and Technology Development Agency (NSTDA), Thailand Science Research and Innovation (TSRI) and National Science, Research and Innovation Fund (NSRF), Thailand; Turkish Energy, Nuclear and Mineral Research Agency (TENMAK), Turkey; National Academy of Sciences of Ukraine, Ukraine; Science and Technology Facilities Council (STFC), United Kingdom; National Science Foundation of the United States of America (NSF) and United States Department of Energy, Office of Nuclear Physics (DOE NP), United States of America. In addition, individual groups or members have received support from: Eu-

ropean Research Council, Strong 2020 - Horizon 2020 (grant nos. 950692, 824093), European Union; Academy of Finland (Center of Excellence in Quark Matter) (grant nos. 346327, 346328), Finland;

References

- [1] W. Busza, K. Rajagopal, and W. van der Schee, “Heavy Ion Collisions: The Big Picture, and the Big Questions”, *Ann. Rev. Nucl. Part. Sci.* **68** (2018) 339–376, arXiv:1802.04801 [hep-ph].
- [2] **HotQCD** Collaboration, A. Bazavov *et al.*, “Equation of state in (2+1)-flavor QCD”, *Phys. Rev. D* **90** (2014) 094503, arXiv:1407.6387 [hep-lat].
- [3] C. Ratti, “Lattice QCD and heavy ion collisions: a review of recent progress”, *Rept. Prog. Phys.* **81** (2018) 084301, arXiv:1804.07810 [hep-lat].
- [4] **ALICE** Collaboration, “The ALICE experiment - A journey through QCD”, arXiv:2211.04384 [nucl-ex].
- [5] M. Gyulassy and M. Plumer, “Jet Quenching in Dense Matter”, *Phys. Lett. B* **243** (1990) 432–438.
- [6] G.-Y. Qin and X.-N. Wang, “Jet quenching in high-energy heavy-ion collisions”, *Int. J. Mod. Phys. E* **24** (2015) 1530014, arXiv:1511.00790 [hep-ph].
- [7] M. Connors, C. Nattrass, R. Reed, and S. Salur, “Jet measurements in heavy ion physics”, *Rev. Mod. Phys.* **90** (2018) 025005, arXiv:1705.01974 [nucl-ex].
- [8] **ALICE** Collaboration, S. Acharya *et al.*, “Measurements of inclusive jet spectra in pp and central Pb-Pb collisions at $\sqrt{s_{\text{NN}}} = 5.02$ TeV”, *Phys. Rev. C* **101** (2020) 034911, arXiv:1909.09718 [nucl-ex].
- [9] **STAR** Collaboration, J. Adam *et al.*, “Measurement of inclusive charged-particle jet production in Au+Au collisions at $\sqrt{s_{\text{NN}}} = 200$ GeV”, *Phys. Rev. C* **102** (2020) 054913, arXiv:2006.00582 [nucl-ex].
- [10] **CMS** Collaboration, V. Khachatryan *et al.*, “Measurement of inclusive jet cross sections in pp and PbPb collisions at $\sqrt{s_{\text{NN}}} = 2.76$ TeV”, *Phys. Rev. C* **96** (2017) 015202, arXiv:1609.05383 [nucl-ex].
- [11] **ATLAS** Collaboration, G. Aad *et al.*, “Measurements of the Nuclear Modification Factor for Jets in Pb+Pb Collisions at $\sqrt{s_{\text{NN}}} = 2.76$ TeV with the ATLAS Detector”, *Phys. Rev. Lett.* **114** (2015) 072302, arXiv:1411.2357 [hep-ex].
- [12] R. Baier, Y. L. Dokshitzer, A. H. Mueller, S. Peigne, and D. Schiff, “Radiative energy loss of high-energy quarks and gluons in a finite volume quark-gluon plasma”, *Nucl. Phys. B* **483** (1997) 291–320, arXiv:hep-ph/9607355.
- [13] M. Gyulassy, P. Levai, and I. Vitev, “NonAbelian energy loss at finite opacity”, *Phys. Rev. Lett.* **85** (2000) 5535–5538, arXiv:nucl-th/0005032.
- [14] M. Djordjevic, D. Zicic, M. Djordjevic, and J. Auvinen, “How to test path-length dependence in energy loss mechanisms: analysis leading to a new observable”, *Phys. Rev. C* **99** (2019) 061902, arXiv:1805.04030 [nucl-th].
- [15] M. Djordjevic and M. Gyulassy, “Heavy quark radiative energy loss in QCD matter”, *Nucl. Phys. A* **733** (2004) 265–298, arXiv:nucl-th/0310076.

- [16] **ATLAS** Collaboration, G. Aad *et al.*, “Observation of a Centrality-Dependent Dijet Asymmetry in Lead-Lead Collisions at $\sqrt{s_{\text{NN}}} = 2.76$ TeV with the ATLAS Detector at the LHC”, *Phys. Rev. Lett.* **105** (2010) 252303, arXiv:1011.6182 [hep-ex].
- [17] **ATLAS** Collaboration, G. Aad *et al.*, “Measurements of the suppression and correlations of dijets in Pb+Pb collisions at $\sqrt{s_{\text{NN}}} = 5.02$ TeV”, *Phys. Rev. C* **107** (2023) 054908, arXiv:2205.00682 [nucl-ex].
- [18] **CMS** Collaboration, S. Chatrchyan *et al.*, “Observation and studies of jet quenching in PbPb collisions at nucleon-nucleon center-of-mass energy = 2.76 TeV”, *Phys. Rev. C* **84** (2011) 024906, arXiv:1102.1957 [nucl-ex].
- [19] J. G. Milhano and K. C. Zapp, “Origins of the di-jet asymmetry in heavy ion collisions”, *Eur. Phys. J. C* **76** (2016) 288, arXiv:1512.08107 [hep-ph].
- [20] **ALICE** Collaboration, J. Adam *et al.*, “Azimuthal anisotropy of charged jet production in $\sqrt{s_{\text{NN}}} = 2.76$ TeV Pb–Pb collisions”, *Phys. Lett. B* **753** (2016) 511–525, arXiv:1509.07334 [nucl-ex].
- [21] **ATLAS** Collaboration, G. Aad *et al.*, “Measurement of the Azimuthal Angle Dependence of Inclusive Jet Yields in Pb+Pb Collisions at $\sqrt{s_{\text{NN}}} = 2.76$ TeV with the ATLAS detector”, *Phys. Rev. Lett.* **111** (2013) 152301, arXiv:1306.6469 [hep-ex].
- [22] **ATLAS** Collaboration, G. Aad *et al.*, “Measurements of azimuthal anisotropies of jet production in Pb+Pb collisions at $\sqrt{s_{\text{NN}}} = 5.02$ TeV with the ATLAS detector”, *Phys. Rev. C* **105** (2022) 064903, arXiv:2111.06606 [nucl-ex].
- [23] J. Schukraft, A. Timmins, and S. A. Voloshin, “Ultra-relativistic nuclear collisions: event shape engineering”, *Phys. Lett. B* **719** (2013) 394–398, arXiv:1208.4563 [nucl-ex].
- [24] P. Christiansen, “Event-Shape Engineering and Jet Quenching”, *J. Phys. Conf. Ser.* **736** (2016) 012023, arXiv:1606.07963 [hep-ph].
- [25] **ALICE** Collaboration, J. Adam *et al.*, “Event shape engineering for inclusive spectra and elliptic flow in Pb–Pb collisions at $\sqrt{s_{\text{NN}}} = 2.76$ TeV”, *Phys. Rev. C* **93** (2016) 034916, arXiv:1507.06194 [nucl-ex].
- [26] **ALICE** Collaboration, S. Acharya *et al.*, “Constraining the magnitude of the Chiral Magnetic Effect with Event Shape Engineering in Pb–Pb collisions at $\sqrt{s_{\text{NN}}} = 2.76$ TeV”, *Phys. Lett. B* **777** (2018) 151–162, arXiv:1709.04723 [nucl-ex].
- [27] **ATLAS** Collaboration, G. Aad *et al.*, “Measurement of the correlation between flow harmonics of different order in lead-lead collisions at $\sqrt{s_{\text{NN}}} = 2.76$ TeV with the ATLAS detector”, *Phys. Rev. C* **92** (2015) 034903, arXiv:1504.01289 [hep-ex].
- [28] **ALICE** Collaboration, S. Acharya *et al.*, “Event-shape engineering for the D-meson elliptic flow in mid-central Pb–Pb collisions at $\sqrt{s_{\text{NN}}} = 5.02$ TeV”, *JHEP* **02** (2019) 150, arXiv:1809.09371 [nucl-ex].
- [29] **ALICE** Collaboration, S. Acharya *et al.*, “Transverse-momentum and event-shape dependence of D-meson flow harmonics in Pb–Pb collisions at $\sqrt{s_{\text{NN}}} = 5.02$ TeV”, *Phys. Lett. B* **813** (2021) 136054, arXiv:2005.11131 [nucl-ex].
- [30] C. Beattie, G. Nijs, M. Sas, and W. van der Schee, “Hard probe path lengths and event-shape engineering of the quark-gluon plasma”, *Phys. Lett. B* **836** (2023) 137596, arXiv:2203.13265 [nucl-th].

- [31] ALICE Collaboration, “Centrality determination in heavy ion collisions”, 2018. <https://cds.cern.ch/record/2636623>.
- [32] ALICE Collaboration, K. Aamodt *et al.*, “The ALICE experiment at the CERN LHC”, *JINST* **3** (2008) S08002.
- [33] ALICE Collaboration, B. Abelev *et al.*, “Performance of the ALICE Experiment at the CERN LHC”, *Int. J. Mod. Phys. A* **29** (2014) 1430044, arXiv:1402.4476 [nucl-ex].
- [34] ALICE Collaboration, K. Aamodt *et al.*, “Alignment of the ALICE Inner Tracking System with cosmic-ray tracks”, *JINST* **5** (2010) P03003, arXiv:1001.0502 [physics.ins-det].
- [35] J. Alme *et al.*, “The ALICE TPC, a large 3-dimensional tracking device with fast readout for ultra-high multiplicity events”, *Nucl. Instrum. Meth. A* **622** (2010) 316–367, arXiv:1001.1950 [physics.ins-det].
- [36] ALICE Collaboration, P. Cortese *et al.*, “ALICE technical design report on forward detectors: FMD, T0 and V0”, 2004. <https://cds.cern.ch/record/781854>.
- [37] ALICE Collaboration, E. Abbas *et al.*, “Performance of the ALICE VZERO system”, *JINST* **8** (2013) P10016, arXiv:1306.3130 [nucl-ex].
- [38] ALICE Collaboration, B. Abelev *et al.*, “Measurement of Event Background Fluctuations for Charged Particle Jet Reconstruction in Pb–Pb collisions at $\sqrt{s_{\text{NN}}} = 2.76 \text{ TeV}$ ”, *JHEP* **03** (2012) 053, arXiv:1201.2423 [hep-ex].
- [39] M. Cacciari, G. P. Salam, and G. Soyez, “FastJet User Manual”, *Eur. Phys. J. C* **72** (2012) 1896, arXiv:1111.6097 [hep-ph].
- [40] M. Cacciari, G. P. Salam, and G. Soyez, “The anti- k_t jet clustering algorithm”, *JHEP* **04** (2008) 063, arXiv:0802.1189 [hep-ph].
- [41] OPAL Collaboration, M. Z. Akrawy *et al.*, “A Study of the recombination scheme dependence of jet production rates and of $\alpha_s(M_{Z^0})$ in hadronic Z^0 decays”, *Z. Phys. C* **49** (1991) 375–384.
- [42] M. Cacciari and G. P. Salam, “Pileup subtraction using jet areas”, *Phys. Lett. B* **659** (2008) 119–126, arXiv:0707.1378 [hep-ph].
- [43] M. Cacciari, J. Rojo, G. P. Salam, and G. Soyez, “Jet Reconstruction in Heavy Ion Collisions”, *Eur. Phys. J. C* **71** (2011) 1539, arXiv:1010.1759 [hep-ph].
- [44] S. D. Ellis and D. E. Soper, “Successive combination jet algorithm for hadron collisions”, *Phys. Rev. D* **48** (1993) 3160–3166, arXiv:hep-ph/9305266.
- [45] G. D’Agostini, “A multidimensional unfolding method based on Bayes’ theorem”, *Nucl. Instrum. Meth. A* **362** (1995) 487–498.
- [46] T. Adye, “Unfolding algorithms and tests using RooUnfold”, in *Proceedings of the PHYSTAT 2011 Workshop*, pp. 313–318. CERN, Geneva, 2011. arXiv:1105.1160 [physics.data-an].
- [47] T. Sjöstrand *et al.*, “An introduction to PYTHIA 8.2”, *Comput. Phys. Commun.* **191** (2015) 159–177, arXiv:1410.3012 [hep-ph].
- [48] P. Skands, S. Carrazza, and J. Rojo, “Tuning PYTHIA 8.1: the Monash 2013 Tune”, *Eur. Phys. J. C* **74** (2014) 3024, arXiv:1404.5630 [hep-ph].

- [49] R. Brun et al., “GEANT Detector Description and Simulation Tool”, 1994.
<https://cds.cern.ch/record/1082634>.
- [50] M. Gyulassy and X.-N. Wang, “HIJING 1.0: A Monte Carlo program for parton and particle production in high-energy hadronic and nuclear collisions”, *Comput. Phys. Commun.* **83** (1994) 307, [arXiv:nucl-th/9502021](https://arxiv.org/abs/nucl-th/9502021).
- [51] **STAR** Collaboration, C. Adler *et al.*, “Elliptic flow from two and four particle correlations in Au+Au collisions at $\sqrt{s_{\text{NN}}} = 130$ GeV”, *Phys. Rev. C* **66** (2002) 034904, [arXiv:nucl-ex/0206001](https://arxiv.org/abs/nucl-ex/0206001).
- [52] S. Voloshin and Y. Zhang, “Flow study in relativistic nuclear collisions by Fourier expansion of Azimuthal particle distributions”, *Z. Phys. C* **70** (1996) 665–672, [arXiv:hep-ph/9407282](https://arxiv.org/abs/hep-ph/9407282).
- [53] A. Poskanzer and S. Voloshin, “Methods for analyzing anisotropic flow in relativistic nuclear collisions”, *Phys. Rev. C* **58** (1998) 1671–1678.
- [54] G. Nijs, W. van der Schee, U. Gürsoy, and R. Snellings, “Bayesian analysis of heavy ion collisions with the heavy ion computational framework Trajectum”, *Phys. Rev. C* **103** (2021) 054909, [arXiv:2010.15134 \[nucl-th\]](https://arxiv.org/abs/2010.15134).
- [55] **ALICE** Collaboration, “Measurement of the radius dependence of charged-particle jet suppression in Pb–Pb collisions at $\sqrt{s_{\text{NN}}} = 5.02$ TeV”, [arXiv:2303.00592 \[nucl-ex\]](https://arxiv.org/abs/2303.00592).
- [56] Y. He, T. Luo, X.-N. Wang, and Y. Zhu, “Linear Boltzmann Transport for Jet Propagation in the Quark-Gluon Plasma: Elastic Processes and Medium Recoil”, *Phys. Rev. C* **91** (2015) 054908, [arXiv:1503.03313 \[nucl-th\]](https://arxiv.org/abs/1503.03313). [Erratum: *Phys. Rev. C* 97, 019902 (2018)].
- [57] Y. He, S. Cao, W. Chen, T. Luo, L.-G. Pang, and X.-N. Wang, “Interplaying mechanisms behind single inclusive jet suppression in heavy-ion collisions”, *Phys. Rev. C* **99** (2019) 054911, [arXiv:1809.02525 \[nucl-th\]](https://arxiv.org/abs/1809.02525).
- [58] J. H. Putschke *et al.*, “The JETSCAPE framework”, [arXiv:1903.07706 \[nucl-th\]](https://arxiv.org/abs/1903.07706).
- [59] L. Barreto, F. M. Canedo, M. G. Munhoz, J. Noronha, and J. Noronha-Hostler, “Jet cone radius dependence of R_{AA} and v_2 at PbPb 5.02 TeV from JEWEL+T_RENTo+v-USPhydro”, [arXiv:2208.02061 \[nucl-th\]](https://arxiv.org/abs/2208.02061).
- [60] I. Kolb  , “JEWEL on a (2+1)D background with applications to small systems and substructure”, [arXiv:2303.14166 \[nucl-th\]](https://arxiv.org/abs/2303.14166).

A The ALICE Collaboration

S. Acharya ¹²⁶, D. Adamová ⁸⁶, G. Aglieri Rinella ³³, M. Agnello ³⁰, N. Agrawal ⁵¹, Z. Ahammed ¹³⁴, S. Ahmad ¹⁶, S.U. Ahn ⁷¹, I. Ahuja ³⁸, A. Akindinov ¹⁴², M. Al-Turany ⁹⁷, D. Aleksandrov ¹⁴², B. Alessandro ⁵⁶, H.M. Alfanda ⁶, R. Alfaro Molina ⁶⁷, B. Ali ¹⁶, A. Alici ²⁶, N. Alizadehvandchali ¹¹⁵, A. Alkin ³³, J. Alme ²¹, G. Alocco ⁵², T. Alt ⁶⁴, A.R. Altamura ⁵⁰, I. Altsybeev ⁹⁵, M.N. Anaam ⁶, C. Andrei ⁴⁶, N. Andreou ¹¹⁴, A. Andronic ¹³⁷, V. Anguelov ⁹⁴, F. Antinori ⁵⁴, P. Antonioli ⁵¹, N. Apadula ⁷⁴, L. Aphecteche ¹⁰³, H. Appelshäuser ⁶⁴, C. Arata ⁷³, S. Arcelli ²⁶, M. Aresti ²³, R. Arnaldi ⁵⁶, J.G.M.C.A. Arneiro ¹¹⁰, I.C. Arsene ²⁰, M. Arslanbekov ¹³⁹, A. Augustinus ³³, R. Averbeck ⁹⁷, M.D. Azmi ¹⁶, H. Baba ¹²³, A. Badala ⁵³, J. Bae ¹⁰⁴, Y.W. Baek ⁴¹, X. Bai ¹¹⁹, R. Bailhache ⁶⁴, Y. Bailung ⁴⁸, A. Balibino ³⁰, A. Baldissari ¹²⁹, B. Balis ², D. Banerjee ⁴, Z. Banoo ⁹¹, R. Barbera ²⁷, F. Barile ³², L. Barioglio ⁹⁵, M. Barlou ⁷⁸, B. Barman ⁴², G.G. Barnaföldi ¹³⁸, L.S. Barnby ⁸⁵, V. Barret ¹²⁶, L. Barreto ¹¹⁰, C. Bartels ¹¹⁸, K. Barth ³³, E. Bartsch ⁶⁴, N. Bastid ¹²⁶, S. Basu ⁷⁵, G. Batigne ¹⁰³, D. Battistini ⁹⁵, B. Batyunya ¹⁴³, D. Bauri ⁴⁷, J.L. Bazo Alba ¹⁰¹, I.G. Bearden ⁸³, C. Beattie ¹³⁹, P. Becht ⁹⁷, D. Behera ⁴⁸, I. Belikov ¹²⁸, A.D.C. Bell Hechavarria ¹³⁷, F. Bellini ²⁶, R. Bellwied ¹¹⁵, S. Belokurova ¹⁴², Y.A.V. Beltran ⁴⁵, G. Bencedi ¹³⁸, S. Beole ²⁵, Y. Berdnikov ¹⁴², A. Berdnikova ⁹⁴, L. Bergmann ⁹⁴, M.G. Besoiu ⁶³, L. Betev ³³, P.P. Bhaduri ¹³⁴, A. Bhasin ⁹¹, M.A. Bhat ⁴, B. Bhattacharjee ⁴², L. Bianchi ²⁵, N. Bianchi ⁴⁹, J. Bielčík ³⁶, J. Bielčíková ⁸⁶, J. Biernat ¹⁰⁷, A.P. Bigot ¹²⁸, A. Bilandzic ⁹⁵, G. Biro ¹³⁸, S. Biswas ⁴, N. Bize ¹⁰³, J.T. Blair ¹⁰⁸, D. Blau ¹⁴², M.B. Blidaru ⁹⁷, N. Bluhme ³⁹, C. Blume ⁶⁴, G. Boca ^{22,55}, F. Bock ⁸⁷, T. Bodova ²¹, A. Bogdanov ¹⁴², S. Boi ²³, J. Bok ⁵⁸, L. Boldizsár ¹³⁸, M. Bombara ³⁸, P.M. Bond ³³, G. Bonomi ^{133,55}, H. Borel ¹²⁹, A. Borissov ¹⁴², A.G. Borquez Carcamo ⁹⁴, H. Bossi ¹³⁹, E. Botta ²⁵, Y.E.M. Bouziani ⁶⁴, L. Bratrud ⁶⁴, P. Braun-Munzinger ⁹⁷, M. Bregant ¹¹⁰, M. Broz ³⁶, G.E. Bruno ^{96,32}, M.D. Buckland ²⁴, D. Budnikov ¹⁴², H. Buesching ⁶⁴, S. Bufalino ³⁰, P. Buhler ¹⁰², N. Burmasov ¹⁴², Z. Buthelezi ^{68,122}, A. Bylinkin ²¹, S.A. Bysiak ¹⁰⁷, M. Cai ⁶, H. Caines ¹³⁹, A. Caliva ²⁹, E. Calvo Villar ¹⁰¹, J.M.M. Camacho ¹⁰⁹, P. Camerini ²⁴, F.D.M. Canedo ¹¹⁰, M. Carabas ¹²⁵, A.A. Carballo ³³, F. Carnesecchi ³³, R. Caron ¹²⁷, L.A.D. Carvalho ¹¹⁰, J. Castillo Castellanos ¹²⁹, F. Catalano ^{33,25}, C. Ceballos Sanchez ¹⁴³, I. Chakaberia ⁷⁴, P. Chakraborty ⁴⁷, S. Chandra ¹³⁴, S. Chapelard ³³, M. Chartier ¹¹⁸, S. Chattopadhyay ¹³⁴, S. Chattopadhyay ⁹⁹, T.G. Chavez ⁴⁵, T. Cheng ^{97,6}, C. Cheshkov ¹²⁷, B. Cheynis ¹²⁷, V. Chibante Barroso ³³, D.D. Chinellato ¹¹¹, E.S. Chizzali ^{I,95}, J. Cho ⁵⁸, S. Cho ⁵⁸, P. Chochula ³³, D. Choudhury ⁴², P. Christakoglou ⁸⁴, C.H. Christensen ⁸³, P. Christiansen ⁷⁵, T. Chujo ¹²⁴, M. Ciaccio ³⁰, C. Cicalo ⁵², F. Cindolo ⁵¹, M.R. Ciupek ⁹⁷, G. Clai ^{II,51}, F. Colamaria ⁵⁰, J.S. Colburn ¹⁰⁰, D. Colella ^{96,32}, M. Colocci ²⁶, M. Concas ^{III,33}, G. Conesa Balbastre ⁷³, Z. Conesa del Valle ¹³⁰, G. Contin ²⁴, J.G. Contreras ³⁶, M.L. Coquet ¹²⁹, P. Cortese ^{132,56}, M.R. Cosentino ¹¹², F. Costa ³³, S. Costanza ^{22,55}, C. Cot ¹³⁰, J. Crkovská ⁹⁴, P. Crochet ¹²⁶, R. Cruz-Torres ⁷⁴, P. Cui ⁶, A. Dainese ⁵⁴, M.C. Danisch ⁹⁴, A. Danu ⁶³, P. Das ⁸⁰, P. Das ⁴, S. Das ⁴, A.R. Dash ¹³⁷, S. Dash ⁴⁷, R.M.H. David ⁴⁵, A. De Caro ²⁹, G. de Cataldo ⁵⁰, J. de Cuveland ³⁹, A. De Falco ²³, D. De Gruttola ²⁹, N. De Marco ⁵⁶, C. De Martin ²⁴, S. De Pasquale ²⁹, R. Deb ¹³³, R. Del Grande ⁹⁵, L. Dello Stritto ²⁹, W. Deng ⁶, P. Dhankher ¹⁹, D. Di Bari ³², A. Di Mauro ³³, B. Diab ¹²⁹, R.A. Diaz ^{143,7}, T. Dietel ¹¹³, Y. Ding ⁶, J. Ditzel ⁶⁴, R. Divià ³³, D.U. Dixit ¹⁹, Ø. Djupsland ²¹, U. Dmitrieva ¹⁴², A. Dobrin ⁶³, B. Dönigus ⁶⁴, J.M. Dubinski ¹³⁵, A. Dubla ⁹⁷, S. Dudi ⁹⁰, P. Dupieux ¹²⁶, M. Durkac ¹⁰⁶, N. Dzalaiova ¹³, T.M. Eder ¹³⁷, R.J. Ehlers ⁷⁴, F. Eisenhut ⁶⁴, R. Ejima ⁹², D. Elia ⁵⁰, B. Erazmus ¹⁰³, F. Ercolelli ²⁶, F. Erhardt ⁸⁹, M.R. Ersdal ²¹, B. Espagnon ¹³⁰, G. Eulisse ³³, D. Evans ¹⁰⁰, S. Evdokimov ¹⁴², L. Fabbietti ⁹⁵, M. Faggin ²⁸, J. Faivre ⁷³, F. Fan ⁶, W. Fan ⁷⁴, A. Fantoni ⁴⁹, M. Fasel ⁸⁷, P. Fecchio ³⁰, A. Feliciello ⁵⁶, G. Feofilov ¹⁴², A. Fernández Téllez ⁴⁵, L. Ferrandi ¹¹⁰, M.B. Ferrer ³³, A. Ferrero ¹²⁹, C. Ferrero ⁵⁶, A. Ferretti ²⁵, V.J.G. Feuillard ⁹⁴, V. Filova ³⁶, D. Finogeev ¹⁴², F.M. Fionda ⁵², F. Flor ¹¹⁵, A.N. Flores ¹⁰⁸, S. Foertsch ⁶⁸, I. Fokin ⁹⁴, S. Fokin ¹⁴², E. Fragiaco ⁵⁷, E. Frajna ¹³⁸, U. Fuchs ³³, N. Funicello ²⁹, C. Furget ⁷³, A. Furs ¹⁴², T. Fusayasu ⁹⁸, J.J. Gaardhøje ⁸³, M. Gagliardi ²⁵, A.M. Gago ¹⁰¹, T. Gahlaut ⁴⁷, C.D. Galvan ¹⁰⁹, D.R. Gangadharan ¹¹⁵, P. Ganoti ⁷⁸, C. Garabatos ⁹⁷, A.T. Garcia ¹³⁰, J.R.A. Garcia ⁴⁵, E. Garcia-Solis ⁹, C. Gargiulo ³³, P. Gasik ⁹⁷, A. Gautam ¹¹⁷, M.B. Gay Ducati ⁶⁶, M. Germain ¹⁰³, A. Ghimouz ¹²⁴, C. Ghosh ¹³⁴, M. Giacalone ⁵¹, G. Gioachin ³⁰, P. Giubellino ^{97,56}, P. Giubilato ²⁸, A.M.C. Glaenzer ¹²⁹, P. Glässel ⁹⁴, E. Glimos ¹²¹, D.J.Q. Goh ⁷⁶, V. Gonzalez ¹³⁶, M. Gorgon ², K. Goswami ⁴⁸, S. Gotovac ³⁴, V. Grabski ⁶⁷, L.K. Graczykowski ¹³⁵, E. Grecka ⁸⁶, A. Grelli ⁵⁹, C. Grigoras ³³, V. Grigoriev ¹⁴², S. Grigoryan ^{143,1}, F. Grossa ³³, J.F. Grosse-Oetringhaus ³³, R. Grossi ⁹⁷, D. Grund ³⁶, N.A. Grunwald ⁹⁴, G.G. Guardiano ¹¹¹,

- R. Guernane ⁷³, M. Guilbaud ¹⁰³, K. Gulbrandsen ⁸³, T. Gundem ⁶⁴, T. Gunji ¹²³, W. Guo ⁶,
 A. Gupta ⁹¹, R. Gupta ⁹¹, R. Gupta ⁴⁸, S.P. Guzman ⁴⁵, K. Gwizdziel ¹³⁵, L. Gyulai ¹³⁸,
 C. Hadjidakis ¹³⁰, F.U. Haider ⁹¹, S. Haidlova ³⁶, H. Hamagaki ⁷⁶, A. Hamdi ⁷⁴, Y. Han ¹⁴⁰,
 B.G. Hanley ¹³⁶, R. Hannigan ¹⁰⁸, J. Hansen ⁷⁵, M.R. Haque ¹³⁵, J.W. Harris ¹³⁹, A. Harton ⁹,
 H. Hassan ¹¹⁶, D. Hatzifotiadou ⁵¹, P. Hauer ⁴³, L.B. Havener ¹³⁹, S.T. Heckel ⁹⁵, E. Hellbär ⁹⁷,
 H. Helstrup ³⁵, M. Hemmer ⁶⁴, T. Herman ³⁶, G. Herrera Corral ⁸, F. Herrmann ¹³⁷, S. Herrmann ¹²⁷,
 K.F. Hetland ³⁵, B. Heybeck ⁶⁴, H. Hillemanns ³³, B. Hippolyte ¹²⁸, F.W. Hoffmann ⁷⁰, B. Hofman ⁵⁹,
 G.H. Hong ¹⁴⁰, M. Horst ⁹⁵, A. Horzyk ², Y. Hou ⁶, P. Hristov ³³, C. Hughes ¹²¹, P. Huhn ⁶⁴,
 L.M. Huhta ¹¹⁶, T.J. Humanic ⁸⁸, A. Hutson ¹¹⁵, D. Hutter ³⁹, R. Ilkaev ¹⁴², H. Ilyas ¹⁴, M. Inaba ¹²⁴,
 G.M. Innocenti ³³, M. Ippolitov ¹⁴², A. Isakov ^{84,86}, T. Isidori ¹¹⁷, M.S. Islam ⁹⁹, M. Ivanov ¹³,
 M. Ivanov ⁹⁷, V. Ivanov ¹⁴², K.E. Iversen ⁷⁵, M. Jablonski ², B. Jacak ⁷⁴, N. Jacazio ²⁶,
 P.M. Jacobs ⁷⁴, S. Jadlovska ¹⁰⁶, J. Jadlovsky ¹⁰⁶, S. Jaelani ⁸², C. Jahnke ¹¹¹, M.J. Jakubowska ¹³⁵,
 M.A. Janik ¹³⁵, T. Janson ⁷⁰, S. Ji ¹⁷, S. Jia ¹⁰, A.A.P. Jimenez ⁶⁵, F. Jonas ⁸⁷, D.M. Jones ¹¹⁸,
 J.M. Jowett ^{33,97}, J. Jung ⁶⁴, M. Jung ⁶⁴, A. Junique ³³, A. Jusko ¹⁰⁰, M.J. Kabus ^{33,135}, J. Kaewjai ¹⁰⁵,
 P. Kalinak ⁶⁰, A.S. Kalteyer ⁹⁷, A. Kalweit ³³, V. Kaplin ¹⁴², A. Karasu Uysal ⁷², D. Karatovic ⁸⁹,
 O. Karavichev ¹⁴², T. Karavicheva ¹⁴², P. Karczmarczyk ¹³⁵, E. Karpechev ¹⁴², U. Kebschull ⁷⁰,
 R. Keidel ¹⁴¹, D.L.D. Keijdener ⁵⁹, M. Keil ³³, B. Ketzer ⁴³, S.S. Khade ⁴⁸, A.M. Khan ^{119,6},
 S. Khan ¹⁶, A. Khanzadeev ¹⁴², Y. Kharlov ¹⁴², A. Khatun ¹¹⁷, A. Khuntia ³⁶, B. Kileng ³⁵,
 B. Kim ¹⁰⁴, C. Kim ¹⁷, D.J. Kim ¹¹⁶, E.J. Kim ⁶⁹, J. Kim ¹⁴⁰, J.S. Kim ⁴¹, J. Kim ⁵⁸, J. Kim ⁶⁹,
 M. Kim ¹⁹, S. Kim ¹⁸, T. Kim ¹⁴⁰, K. Kimura ⁹², S. Kirsch ⁶⁴, I. Kisel ³⁹, S. Kiselev ¹⁴²,
 A. Kisiel ¹³⁵, J.P. Kitowski ², J.L. Klay ⁵, J. Klein ³³, S. Klein ⁷⁴, C. Klein-Bösing ¹³⁷,
 M. Kleiner ⁶⁴, T. Klemenz ⁹⁵, A. Kluge ³³, A.G. Knospe ¹¹⁵, C. Kobdaj ¹⁰⁵, T. Kollegger ⁹⁷,
 A. Kondratyev ¹⁴³, N. Kondratyeva ¹⁴², E. Kondratyuk ¹⁴², J. Konig ⁶⁴, S.A. Konigstorfer ⁹⁵,
 P.J. Konopka ³³, G. Kornakov ¹³⁵, S.D. Koryciak ², A. Kotliarov ⁸⁶, V. Kovalenko ¹⁴²,
 M. Kowalski ¹⁰⁷, V. Kozhuharov ³⁷, I. Králik ⁶⁰, A. Kravčáková ³⁸, L. Krcal ^{33,39}, M. Krivda ^{100,60},
 F. Krizek ⁸⁶, K. Krizkova Gajdosova ³³, M. Kroesen ⁹⁴, M. Krüger ⁶⁴, D.M. Krupova ³⁶,
 E. Kryshen ¹⁴², V. Kučera ⁵⁸, C. Kuhn ¹²⁸, P.G. Kuijer ⁸⁴, T. Kumaoka ¹²⁴, D. Kumar ¹³⁴, L. Kumar ⁹⁰,
 N. Kumar ⁹⁰, S. Kumar ³², S. Kundu ³³, P. Kurashvili ⁷⁹, A. Kurepin ¹⁴², A.B. Kurepin ¹⁴²,
 A. Kuryakin ¹⁴², S. Kushpil ⁸⁶, M.J. Kweon ⁵⁸, Y. Kwon ¹⁴⁰, S.L. La Pointe ³⁹, P. La Rocca ²⁷,
 A. Lakhathok ¹⁰⁵, M. Lamanna ³³, R. Langoy ¹²⁰, P. Larionov ³³, E. Laudi ³³, L. Lautner ^{33,95},
 R. Lavicka ¹⁰², R. Lea ^{133,55}, H. Lee ¹⁰⁴, I. Legrand ⁴⁶, G. Legras ¹³⁷, J. Lehrbach ³⁹, T.M. Lelek ²,
 R.C. Lemmon ⁸⁵, I. León Monzón ¹⁰⁹, M.M. Lesch ⁹⁵, E.D. Lesser ¹⁹, P. Lévai ¹³⁸, X. Li ¹⁰,
 J. Lien ¹²⁰, R. Lietava ¹⁰⁰, I. Likmeta ¹¹⁵, B. Lim ²⁵, S.H. Lim ¹⁷, V. Lindenstruth ³⁹, A. Lindner ⁴⁶,
 C. Lippmann ⁹⁷, D.H. Liu ⁶, J. Liu ¹¹⁸, G.S.S. Liveraro ¹¹¹, I.M. Lofnes ²¹, C. Loizides ⁸⁷,
 S. Lokos ¹⁰⁷, J. Lomker ⁵⁹, P. Loncar ³⁴, X. Lopez ¹²⁶, E. López Torres ⁷, P. Lu ^{97,119},
 J.R. Luhder ¹³⁷, M. Lunardon ²⁸, G. Luparello ⁵⁷, Y.G. Ma ⁴⁰, M. Mager ³³, A. Maire ¹²⁸,
 M.V. Makariev ³⁷, M. Malaev ¹⁴², G. Malfattore ²⁶, N.M. Malik ⁹¹, Q.W. Malik ²⁰, S.K. Malik ⁹¹,
 L. Malinina ^{VI,143}, D. Mallick ^{130,80}, N. Mallick ⁴⁸, G. Mandaglio ^{31,53}, S.K. Mandal ⁷⁹, V. Manko ¹⁴²,
 F. Manso ¹²⁶, V. Manzari ⁵⁰, Y. Mao ⁶, R.W. Marcjan ², G.V. Margagliotti ²⁴, A. Margotti ⁵¹,
 A. Marín ⁹⁷, C. Markert ¹⁰⁸, P. Martinengo ³³, M.I. Martínez ⁴⁵, G. Martínez García ¹⁰³,
 M.P.P. Martins ¹¹⁰, S. Masciocchi ⁹⁷, M. Masera ²⁵, A. Masoni ⁵², L. Massacrier ¹³⁰, O. Massen ⁵⁹,
 A. Mastroserio ^{131,50}, O. Matonoha ⁷⁵, S. Mattiuzzo ²⁸, A. Matyja ¹⁰⁷, C. Mayer ¹⁰⁷,
 A.L. Mazuecos ³³, F. Mazzaschi ²⁵, M. Mazzilli ³³, J.E. Mdhluli ¹²², Y. Melikyan ⁴⁴,
 A. Menchaca-Rocha ⁶⁷, E. Meninno ^{102,29}, A.S. Menon ¹¹⁵, M. Meres ¹³, S. Mhlanga ^{113,68}, Y. Miake ¹²⁴,
 L. Micheletti ³³, D.L. Mihaylov ⁹⁵, K. Mikhaylov ^{143,142}, A.N. Mishra ¹³⁸, D. Miśkowiec ⁹⁷,
 A. Modak ⁴, B. Mohanty ⁸⁰, M. Mohisin Khan ^{IV,16}, M.A. Molander ⁴⁴, S. Monira ¹³⁵, C. Mordasini ¹¹⁶,
 D.A. Moreira De Godoy ¹³⁷, I. Morozov ¹⁴², A. Morsch ³³, T. Mrnjavac ³³, V. Muccifora ⁴⁹,
 S. Muhuri ¹³⁴, J.D. Mulligan ⁷⁴, A. Mulliri ²³, M.G. Munhoz ¹¹⁰, R.H. Munzer ⁶⁴, H. Murakami ¹²³,
 S. Murray ¹¹³, L. Musa ³³, J. Musinsky ⁶⁰, J.W. Myrcha ¹³⁵, B. Naik ¹²², A.I. Nambrath ¹⁹,
 B.K. Nandi ⁴⁷, R. Nania ⁵¹, E. Nappi ⁵⁰, A.F. Nassirpour ¹⁸, A. Nath ⁹⁴, C. Nattrass ¹²¹,
 M.N. Naydenov ³⁷, A. Neagu ²⁰, A. Negru ¹²⁵, L. Nellen ⁶⁵, R. Nepeivoda ⁷⁵, S. Nese ²⁰, G. Neskovic ³⁹,
 N. Nicassio ⁵⁰, B.S. Nielsen ⁸³, E.G. Nielsen ⁸³, S. Nikolaev ¹⁴², S. Nikulin ¹⁴², V. Nikulin ¹⁴²,
 F. Noferini ⁵¹, S. Noh ¹², P. Nomokonov ¹⁴³, J. Norman ¹¹⁸, N. Novitzky ¹²⁴, P. Nowakowski ¹³⁵,
 A. Nyanin ¹⁴², J. Nystrand ²¹, M. Ogino ⁷⁶, S. Oh ¹⁸, A. Ohlson ⁷⁵, V.A. Okorokov ¹⁴²,
 J. Oleniacz ¹³⁵, A.C. Oliveira Da Silva ¹²¹, A. Onnerstad ¹¹⁶, C. Oppedisano ⁵⁶, A. Ortiz Velasquez ⁶⁵,
 J. Otwinowski ¹⁰⁷, M. Oya ⁹², K. Oyama ⁷⁶, Y. Pachmayer ⁹⁴, S. Padhan ⁴⁷, D. Pagano ^{133,55},

- G. Paić ⁶⁵, A. Palasciano ⁵⁰, S. Panebianco ¹²⁹, H. Park ¹²⁴, H. Park ¹⁰⁴, J. Park ⁵⁸, J.E. Parkkila ³³, Y. Patley ⁴⁷, R.N. Patra ⁹¹, B. Paul ²³, H. Pei ⁶, T. Peitzmann ⁵⁹, X. Peng ¹¹, M. Pennisi ²⁵, S. Perciballi ²⁵, D. Peresunko ¹⁴², G.M. Perez ⁷, Y. Pestov ¹⁴², V. Petrov ¹⁴², M. Petrovici ⁴⁶, R.P. Pezzi ^{103,66}, S. Piano ⁵⁷, M. Pikna ¹³, P. Pillot ¹⁰³, O. Pinazza ^{51,33}, L. Pinsky ¹¹⁵, C. Pinto ⁹⁵, S. Pisano ⁴⁹, M. Płoskoń ⁷⁴, M. Planinic ⁸⁹, F. Pliquet ⁶⁴, M.G. Poghosyan ⁸⁷, B. Polichtchouk ¹⁴², S. Politano ³⁰, N. Poljak ⁸⁹, A. Pop ⁴⁶, S. Porteboeuf-Houssais ¹²⁶, V. Pozdniakov ¹⁴³, I.Y. Pozos ⁴⁵, K.K. Pradhan ⁴⁸, S.K. Prasad ⁴, S. Prasad ⁴⁸, R. Preghenella ⁵¹, F. Prino ⁵⁶, C.A. Pruneau ¹³⁶, I. Pshenichnov ¹⁴², M. Puccio ³³, S. Pucillo ²⁵, Z. Pugelova ¹⁰⁶, S. Qiu ⁸⁴, L. Quaglia ²⁵, S. Ragoni ¹⁵, A. Rai ¹³⁹, A. Rakotozafindrabe ¹²⁹, L. Ramello ^{132,56}, F. Rami ¹²⁸, S.A.R. Ramirez ⁴⁵, T.A. Rancien ⁷³, M. Rasa ²⁷, S.S. Räsänen ⁴⁴, R. Rath ⁵¹, M.P. Rauch ²¹, I. Ravasenga ⁸⁴, K.F. Read ^{87,121}, C. Reckziegel ¹¹², A.R. Redelbach ³⁹, K. Redlich ^{V,79}, C.A. Reetz ⁹⁷, A. Rehman ²¹, F. Reidt ³³, H.A. Reme-Ness ³⁵, Z. Rescakova ³⁸, K. Reygers ⁹⁴, A. Riabov ¹⁴², V. Riabov ¹⁴², R. Ricci ²⁹, M. Richter ²⁰, A.A. Riedel ⁹⁵, W. Riegler ³³, A.G. Riffero ²⁵, C. Ristea ⁶³, M.V. Rodriguez ³³, M. Rodríguez Cahuantzi ⁴⁵, K. Røed ²⁰, R. Rogalev ¹⁴², E. Rogochaya ¹⁴³, T.S. Rogoschinski ⁶⁴, D. Rohr ³³, D. Röhrich ²¹, P.F. Rojas ⁴⁵, S. Rojas Torres ³⁶, P.S. Rokita ¹³⁵, G. Romanenko ²⁶, F. Ronchetti ⁴⁹, A. Rosano ^{31,53}, E.D. Rosas ⁶⁵, K. Roslon ¹³⁵, A. Rossi ⁵⁴, A. Roy ⁴⁸, S. Roy ⁴⁷, N. Rubini ²⁶, O.V. Rueda ¹¹⁵, D. Ruggiano ¹³⁵, R. Rui ²⁴, P.G. Russek ², R. Russo ⁸⁴, A. Rustamov ⁸¹, E. Ryabinkin ¹⁴², Y. Ryabov ¹⁴², A. Rybicki ¹⁰⁷, H. Rytkonen ¹¹⁶, J. Ryu ¹⁷, W. Rzesz ¹³⁵, O.A.M. Saarimaki ⁴⁴, S. Sadhu ³², S. Sadovsky ¹⁴², J. Saetre ²¹, K. Šafařík ³⁶, P. Saha ⁴², S.K. Saha ⁴, S. Saha ⁸⁰, B. Sahoo ⁴⁷, B. Sahoo ⁴⁸, R. Sahoo ⁴⁸, S. Sahoo ⁶¹, D. Sahu ⁴⁸, P.K. Sahu ⁶¹, J. Saini ¹³⁴, K. Sajdakova ³⁸, S. Sakai ¹²⁴, M.P. Salvan ⁹⁷, S. Sambyal ⁹¹, D. Samitz ¹⁰², I. Sanna ^{33,95}, T.B. Saramela ¹¹⁰, P. Sarma ⁴², V. Sarritzu ²³, V.M. Sarti ⁹⁵, M.H.P. Sas ¹³⁹, J. Schambach ⁸⁷, H.S. Scheid ⁶⁴, C. Schiaua ⁴⁶, R. Schicker ⁹⁴, A. Schmeh ⁹⁷, C. Schmidt ⁹⁷, H.R. Schmidt ⁹³, M.O. Schmidt ³³, M. Schmidt ⁹³, N.V. Schmidt ⁸⁷, A.R. Schmier ¹²¹, R. Schotter ¹²⁸, A. Schröter ³⁹, J. Schukraft ³³, K. Schweda ⁹⁷, G. Scioli ²⁶, E. Scopparin ⁵⁶, J.E. Seger ¹⁵, Y. Sekiguchi ¹²³, D. Sekihata ¹²³, M. Selina ⁸⁴, I. Selyuzhenkov ⁹⁷, S. Senyukov ¹²⁸, J.J. Seo ^{94,58}, D. Serebryakov ¹⁴², L. Šerkšnytė ⁹⁵, A. Sevcenco ⁶³, T.J. Shaba ⁶⁸, A. Shabetai ¹⁰³, R. Shahoyan ³³, A. Shangaraev ¹⁴², A. Sharma ⁹⁰, B. Sharma ⁹¹, D. Sharma ⁴⁷, H. Sharma ^{54,107}, M. Sharma ⁹¹, S. Sharma ⁷⁶, S. Sharma ⁹¹, U. Sharma ⁹¹, A. Shatat ¹³⁰, O. Sheibani ¹¹⁵, K. Shigaki ⁹², M. Shimomura ⁷⁷, J. Shin ¹², S. Shirinkin ¹⁴², Q. Shou ⁴⁰, Y. Sibiriak ¹⁴², S. Siddhanta ⁵², T. Siemiaczuk ⁷⁹, T.F. Silva ¹¹⁰, D. Silvermyr ⁷⁵, T. Simantathammakul ¹⁰⁵, R. Simeonov ³⁷, B. Singh ⁹¹, B. Singh ⁹⁵, K. Singh ⁴⁸, R. Singh ⁸⁰, R. Singh ⁹¹, R. Singh ⁴⁸, S. Singh ¹⁶, V.K. Singh ¹³⁴, V. Singhal ¹³⁴, T. Sinha ⁹⁹, B. Sitar ¹³, M. Sitta ^{132,56}, T.B. Skaali ²⁰, G. Skorodumovs ⁹⁴, M. Slupecki ⁴⁴, N. Smirnov ¹³⁹, R.J.M. Snellings ⁵⁹, E.H. Solheim ²⁰, J. Song ¹¹⁵, C. Sonnabend ^{33,97}, F. Soramel ²⁸, A.B. Soto-hernandez ⁸⁸, R. Spijkers ⁸⁴, I. Sputowska ¹⁰⁷, J. Staa ⁷⁵, J. Stachel ⁹⁴, I. Stan ⁶³, P.J. Steffanic ¹²¹, S.F. Stieflmaier ⁹⁴, D. Stocco ¹⁰³, I. Storehaug ²⁰, P. Stratmann ¹³⁷, S. Strazzi ²⁶, A. Sturniolo ^{31,53}, C.P. Stylianidis ⁸⁴, A.A.P. Suáide ¹¹⁰, C. Suire ¹³⁰, M. Sukhanov ¹⁴², M. Suljic ³³, R. Sultanov ¹⁴², V. Sumberia ⁹¹, S. Sumowidagdo ⁸², S. Swain ⁶¹, I. Szarka ¹³, M. Szymkowski ¹³⁵, S.F. Taghavi ⁹⁵, G. Taillepied ⁹⁷, J. Takahashi ¹¹¹, G.J. Tambave ⁸⁰, S. Tang ⁶, Z. Tang ¹¹⁹, J.D. Tapia Takaki ¹¹⁷, N. Tapus ¹²⁵, L.A. Tarasovicova ¹³⁷, M.G. Tarzila ⁴⁶, G.F. Tassielli ³², A. Tauro ³³, G. Tejeda Muñoz ⁴⁵, A. Telesca ³³, L. Terlizzi ²⁵, C. Terrevoli ¹¹⁵, S. Thakur ⁴, D. Thomas ¹⁰⁸, A. Tikhonov ¹⁴², A.R. Timmins ¹¹⁵, M. Tkacik ¹⁰⁶, T. Tkacik ⁶⁴, A. Toia ⁶⁴, R. Tokumoto ⁹², K. Tomohiro ⁹², N. Topilskaya ¹⁴², M. Toppi ⁴⁹, T. Tork ¹³⁰, V.V. Torres ¹⁰³, A.G. Torres Ramos ³², A. Trifirò ^{31,53}, A.S. Triolo ^{33,31,53}, S. Tripathy ⁵¹, T. Tripathy ⁴⁷, S. Trogolo ³³, V. Trubnikov ³, W.H. Trzaska ¹¹⁶, T.P. Trzcinski ¹³⁵, A. Tumkin ¹⁴², R. Turrisi ⁵⁴, T.S. Tveter ²⁰, K. Ullaland ²¹, B. Ulukutlu ⁹⁵, A. Uras ¹²⁷, G.L. Usai ²³, M. Vala ³⁸, N. Valle ²², L.V.R. van Doremalen ⁵⁹, M. van Leeuwen ⁸⁴, C.A. van Veen ⁹⁴, R.J.G. van Weelden ⁸⁴, P. Vande Vyvre ³³, D. Varga ¹³⁸, Z. Varga ¹³⁸, M. Vasileiou ⁷⁸, A. Vasiliev ¹⁴², O. Vázquez Doce ⁴⁹, V. Vechernin ¹⁴², E. Vercellin ²⁵, S. Vergara Limón ⁴⁵, R. Verma ⁴⁷, L. Vermunt ⁹⁷, R. Vértesi ¹³⁸, M. Verweij ⁵⁹, L. Vickovic ³⁴, Z. Vilakazi ¹²², O. Villalobos Baillie ¹⁰⁰, A. Villani ²⁴, A. Vinogradov ¹⁴², T. Virgili ²⁹, M.M.O. Virta ¹¹⁶, V. Vislavicius ⁷⁵, A. Vodopyanov ¹⁴³, B. Volkel ³³, M.A. Völkli ⁹⁴, K. Voloshin ¹⁴², S.A. Voloshin ¹³⁶, G. Volpe ³², B. von Haller ³³, I. Vorobyev ⁹⁵, N. Vozniuk ¹⁴², J. Vrláková ³⁸, J. Wan ⁴⁰, C. Wang ⁴⁰, D. Wang ⁴⁰, Y. Wang ⁴⁰, Y. Wang ⁶, A. Wegrzynek ³³, F.T. Weighofer ³⁹, S.C. Wenzel ³³, J.P. Wessels ¹³⁷, S.L. Weyhmiller ¹³⁹, J. Wiechula ⁶⁴, J. Wikne ²⁰, G. Wilk ⁷⁹, J. Wilkinson ⁹⁷, G.A. Willems ¹³⁷, B. Windelband ⁹⁴, M. Winn ¹²⁹, J.R. Wright ¹⁰⁸, W. Wu ⁴⁰, Y. Wu ¹¹⁹, R. Xu ⁶, A. Yadav ⁴³, A.K. Yadav ¹³⁴, S. Yalcin ⁷², Y. Yamaguchi ⁹², S. Yang ²¹, S. Yano ⁹², Z. Yin ⁶

I.-K. Yoo 17, J.H. Yoon 58, H. Yu¹², S. Yuan²¹, A. Yuncu 94, V. Zaccolo 24, C. Zampolli 33, F. Zanone 94, N. Zardoshti 33, A. Zarochentsev 142, P. Závada 62, N. Zaviyalov¹⁴², M. Zhalov 142, B. Zhang 6, C. Zhang 129, L. Zhang 40, S. Zhang 40, X. Zhang 6, Y. Zhang¹¹⁹, Z. Zhang 6, M. Zhao 10, V. Zherebchevskii 142, Y. Zhi¹⁰, D. Zhou 6, Y. Zhou 83, J. Zhu 97,6, Y. Zhu⁶, S.C. Zugravlel 56, N. Zurlo 133,55

Affiliation Notes

^I Also at: Max-Planck-Institut für Physik, Munich, Germany

^{II} Also at: Italian National Agency for New Technologies, Energy and Sustainable Economic Development (ENEA), Bologna, Italy

^{III} Also at: Dipartimento DET del Politecnico di Torino, Turin, Italy

^{IV} Also at: Department of Applied Physics, Aligarh Muslim University, Aligarh, India

^V Also at: Institute of Theoretical Physics, University of Wroclaw, Poland

^{VI} Also at: An institution covered by a cooperation agreement with CERN

Collaboration Institutes

¹ A.I. Alikhanyan National Science Laboratory (Yerevan Physics Institute) Foundation, Yerevan, Armenia

² AGH University of Science and Technology, Cracow, Poland

³ Bogolyubov Institute for Theoretical Physics, National Academy of Sciences of Ukraine, Kiev, Ukraine

⁴ Bose Institute, Department of Physics and Centre for Astroparticle Physics and Space Science (CAPSS), Kolkata, India

⁵ California Polytechnic State University, San Luis Obispo, California, United States

⁶ Central China Normal University, Wuhan, China

⁷ Centro de Aplicaciones Tecnológicas y Desarrollo Nuclear (CEADEN), Havana, Cuba

⁸ Centro de Investigación y de Estudios Avanzados (CINVESTAV), Mexico City and Mérida, Mexico

⁹ Chicago State University, Chicago, Illinois, United States

¹⁰ China Institute of Atomic Energy, Beijing, China

¹¹ China University of Geosciences, Wuhan, China

¹² Chungbuk National University, Cheongju, Republic of Korea

¹³ Comenius University Bratislava, Faculty of Mathematics, Physics and Informatics, Bratislava, Slovak Republic

¹⁴ COMSATS University Islamabad, Islamabad, Pakistan

¹⁵ Creighton University, Omaha, Nebraska, United States

¹⁶ Department of Physics, Aligarh Muslim University, Aligarh, India

¹⁷ Department of Physics, Pusan National University, Pusan, Republic of Korea

¹⁸ Department of Physics, Sejong University, Seoul, Republic of Korea

¹⁹ Department of Physics, University of California, Berkeley, California, United States

²⁰ Department of Physics, University of Oslo, Oslo, Norway

²¹ Department of Physics and Technology, University of Bergen, Bergen, Norway

²² Dipartimento di Fisica, Università di Pavia, Pavia, Italy

²³ Dipartimento di Fisica dell'Università and Sezione INFN, Cagliari, Italy

²⁴ Dipartimento di Fisica dell'Università and Sezione INFN, Trieste, Italy

²⁵ Dipartimento di Fisica dell'Università and Sezione INFN, Turin, Italy

²⁶ Dipartimento di Fisica e Astronomia dell'Università and Sezione INFN, Bologna, Italy

²⁷ Dipartimento di Fisica e Astronomia dell'Università and Sezione INFN, Catania, Italy

²⁸ Dipartimento di Fisica e Astronomia dell'Università and Sezione INFN, Padova, Italy

²⁹ Dipartimento di Fisica ‘E.R. Caianiello’ dell’Università and Gruppo Collegato INFN, Salerno, Italy

³⁰ Dipartimento DISAT del Politecnico and Sezione INFN, Turin, Italy

³¹ Dipartimento di Scienze MIFT, Università di Messina, Messina, Italy

³² Dipartimento Interateneo di Fisica ‘M. Merlin’ and Sezione INFN, Bari, Italy

³³ European Organization for Nuclear Research (CERN), Geneva, Switzerland

³⁴ Faculty of Electrical Engineering, Mechanical Engineering and Naval Architecture, University of Split, Split, Croatia

³⁵ Faculty of Engineering and Science, Western Norway University of Applied Sciences, Bergen, Norway

- ³⁶ Faculty of Nuclear Sciences and Physical Engineering, Czech Technical University in Prague, Prague, Czech Republic
³⁷ Faculty of Physics, Sofia University, Sofia, Bulgaria
³⁸ Faculty of Science, P.J. Šafárik University, Košice, Slovak Republic
³⁹ Frankfurt Institute for Advanced Studies, Johann Wolfgang Goethe-Universität Frankfurt, Frankfurt, Germany
⁴⁰ Fudan University, Shanghai, China
⁴¹ Gangneung-Wonju National University, Gangneung, Republic of Korea
⁴² Gauhati University, Department of Physics, Guwahati, India
⁴³ Helmholtz-Institut für Strahlen- und Kernphysik, Rheinische Friedrich-Wilhelms-Universität Bonn, Bonn, Germany
⁴⁴ Helsinki Institute of Physics (HIP), Helsinki, Finland
⁴⁵ High Energy Physics Group, Universidad Autónoma de Puebla, Puebla, Mexico
⁴⁶ Horia Hulubei National Institute of Physics and Nuclear Engineering, Bucharest, Romania
⁴⁷ Indian Institute of Technology Bombay (IIT), Mumbai, India
⁴⁸ Indian Institute of Technology Indore, Indore, India
⁴⁹ INFN, Laboratori Nazionali di Frascati, Frascati, Italy
⁵⁰ INFN, Sezione di Bari, Bari, Italy
⁵¹ INFN, Sezione di Bologna, Bologna, Italy
⁵² INFN, Sezione di Cagliari, Cagliari, Italy
⁵³ INFN, Sezione di Catania, Catania, Italy
⁵⁴ INFN, Sezione di Padova, Padova, Italy
⁵⁵ INFN, Sezione di Pavia, Pavia, Italy
⁵⁶ INFN, Sezione di Torino, Turin, Italy
⁵⁷ INFN, Sezione di Trieste, Trieste, Italy
⁵⁸ Inha University, Incheon, Republic of Korea
⁵⁹ Institute for Gravitational and Subatomic Physics (GRASP), Utrecht University/Nikhef, Utrecht, Netherlands
⁶⁰ Institute of Experimental Physics, Slovak Academy of Sciences, Košice, Slovak Republic
⁶¹ Institute of Physics, Homi Bhabha National Institute, Bhubaneswar, India
⁶² Institute of Physics of the Czech Academy of Sciences, Prague, Czech Republic
⁶³ Institute of Space Science (ISS), Bucharest, Romania
⁶⁴ Institut für Kernphysik, Johann Wolfgang Goethe-Universität Frankfurt, Frankfurt, Germany
⁶⁵ Instituto de Ciencias Nucleares, Universidad Nacional Autónoma de México, Mexico City, Mexico
⁶⁶ Instituto de Física, Universidade Federal do Rio Grande do Sul (UFRGS), Porto Alegre, Brazil
⁶⁷ Instituto de Física, Universidad Nacional Autónoma de México, Mexico City, Mexico
⁶⁸ iThemba LABS, National Research Foundation, Somerset West, South Africa
⁶⁹ Jeonbuk National University, Jeonju, Republic of Korea
⁷⁰ Johann-Wolfgang-Goethe Universität Frankfurt Institut für Informatik, Fachbereich Informatik und Mathematik, Frankfurt, Germany
⁷¹ Korea Institute of Science and Technology Information, Daejeon, Republic of Korea
⁷² KTO Karatay University, Konya, Turkey
⁷³ Laboratoire de Physique Subatomique et de Cosmologie, Université Grenoble-Alpes, CNRS-IN2P3, Grenoble, France
⁷⁴ Lawrence Berkeley National Laboratory, Berkeley, California, United States
⁷⁵ Lund University Department of Physics, Division of Particle Physics, Lund, Sweden
⁷⁶ Nagasaki Institute of Applied Science, Nagasaki, Japan
⁷⁷ Nara Women's University (NWU), Nara, Japan
⁷⁸ National and Kapodistrian University of Athens, School of Science, Department of Physics , Athens, Greece
⁷⁹ National Centre for Nuclear Research, Warsaw, Poland
⁸⁰ National Institute of Science Education and Research, Homi Bhabha National Institute, Jatni, India
⁸¹ National Nuclear Research Center, Baku, Azerbaijan
⁸² National Research and Innovation Agency - BRIN, Jakarta, Indonesia
⁸³ Niels Bohr Institute, University of Copenhagen, Copenhagen, Denmark
⁸⁴ Nikhef, National institute for subatomic physics, Amsterdam, Netherlands
⁸⁵ Nuclear Physics Group, STFC Daresbury Laboratory, Daresbury, United Kingdom
⁸⁶ Nuclear Physics Institute of the Czech Academy of Sciences, Husinec-Řež, Czech Republic
⁸⁷ Oak Ridge National Laboratory, Oak Ridge, Tennessee, United States

- ⁸⁸ Ohio State University, Columbus, Ohio, United States
⁸⁹ Physics department, Faculty of science, University of Zagreb, Zagreb, Croatia
⁹⁰ Physics Department, Panjab University, Chandigarh, India
⁹¹ Physics Department, University of Jammu, Jammu, India
⁹² Physics Program and International Institute for Sustainability with Knotted Chiral Meta Matter (SKCM2), Hiroshima University, Hiroshima, Japan
⁹³ Physikalisches Institut, Eberhard-Karls-Universität Tübingen, Tübingen, Germany
⁹⁴ Physikalisches Institut, Ruprecht-Karls-Universität Heidelberg, Heidelberg, Germany
⁹⁵ Physik Department, Technische Universität München, Munich, Germany
⁹⁶ Politecnico di Bari and Sezione INFN, Bari, Italy
⁹⁷ Research Division and ExtreMe Matter Institute EMMI, GSI Helmholtzzentrum für Schwerionenforschung GmbH, Darmstadt, Germany
⁹⁸ Saga University, Saga, Japan
⁹⁹ Saha Institute of Nuclear Physics, Homi Bhabha National Institute, Kolkata, India
¹⁰⁰ School of Physics and Astronomy, University of Birmingham, Birmingham, United Kingdom
¹⁰¹ Sección Física, Departamento de Ciencias, Pontificia Universidad Católica del Perú, Lima, Peru
¹⁰² Stefan Meyer Institut für Subatomare Physik (SMI), Vienna, Austria
¹⁰³ SUBATECH, IMT Atlantique, Nantes Université, CNRS-IN2P3, Nantes, France
¹⁰⁴ Sungkyunkwan University, Suwon City, Republic of Korea
¹⁰⁵ Suranaree University of Technology, Nakhon Ratchasima, Thailand
¹⁰⁶ Technical University of Košice, Košice, Slovak Republic
¹⁰⁷ The Henryk Niewodniczanski Institute of Nuclear Physics, Polish Academy of Sciences, Cracow, Poland
¹⁰⁸ The University of Texas at Austin, Austin, Texas, United States
¹⁰⁹ Universidad Autónoma de Sinaloa, Culiacán, Mexico
¹¹⁰ Universidade de São Paulo (USP), São Paulo, Brazil
¹¹¹ Universidade Estadual de Campinas (UNICAMP), Campinas, Brazil
¹¹² Universidade Federal do ABC, Santo Andre, Brazil
¹¹³ University of Cape Town, Cape Town, South Africa
¹¹⁴ University of Derby, Derby, United Kingdom
¹¹⁵ University of Houston, Houston, Texas, United States
¹¹⁶ University of Jyväskylä, Jyväskylä, Finland
¹¹⁷ University of Kansas, Lawrence, Kansas, United States
¹¹⁸ University of Liverpool, Liverpool, United Kingdom
¹¹⁹ University of Science and Technology of China, Hefei, China
¹²⁰ University of South-Eastern Norway, Kongsberg, Norway
¹²¹ University of Tennessee, Knoxville, Tennessee, United States
¹²² University of the Witwatersrand, Johannesburg, South Africa
¹²³ University of Tokyo, Tokyo, Japan
¹²⁴ University of Tsukuba, Tsukuba, Japan
¹²⁵ University Politehnica of Bucharest, Bucharest, Romania
¹²⁶ Université Clermont Auvergne, CNRS/IN2P3, LPC, Clermont-Ferrand, France
¹²⁷ Université de Lyon, CNRS/IN2P3, Institut de Physique des 2 Infinis de Lyon, Lyon, France
¹²⁸ Université de Strasbourg, CNRS, IPHC UMR 7178, F-67000 Strasbourg, France, Strasbourg, France
¹²⁹ Université Paris-Saclay, Centre d'Etudes de Saclay (CEA), IRFU, Département de Physique Nucléaire (DPhN), Saclay, France
¹³⁰ Université Paris-Saclay, CNRS/IN2P3, IJCLab, Orsay, France
¹³¹ Università degli Studi di Foggia, Foggia, Italy
¹³² Università del Piemonte Orientale, Vercelli, Italy
¹³³ Università di Brescia, Brescia, Italy
¹³⁴ Variable Energy Cyclotron Centre, Homi Bhabha National Institute, Kolkata, India
¹³⁵ Warsaw University of Technology, Warsaw, Poland
¹³⁶ Wayne State University, Detroit, Michigan, United States
¹³⁷ Westfälische Wilhelms-Universität Münster, Institut für Kernphysik, Münster, Germany
¹³⁸ Wigner Research Centre for Physics, Budapest, Hungary
¹³⁹ Yale University, New Haven, Connecticut, United States
¹⁴⁰ Yonsei University, Seoul, Republic of Korea

¹⁴¹ Zentrum für Technologie und Transfer (ZTT), Worms, Germany

¹⁴² Affiliated with an institute covered by a cooperation agreement with CERN

¹⁴³ Affiliated with an international laboratory covered by a cooperation agreement with CERN.